

Stellarator Transport Highlights

D. R. Mikkelsen, M. C. Zarnstorff, S. Gerhardt

Most of the pages are taken from presentations at various meetings by:

**C. Beidler, A. Fujisawa, K. Ida, H. Maassberg, K. McCormick, S. Murakami,
S. Okamura, D. Spong, H. Yamada, M. Yokohama,
and the CHS, LHD, and W7-AS teams**



International Stellarator Database

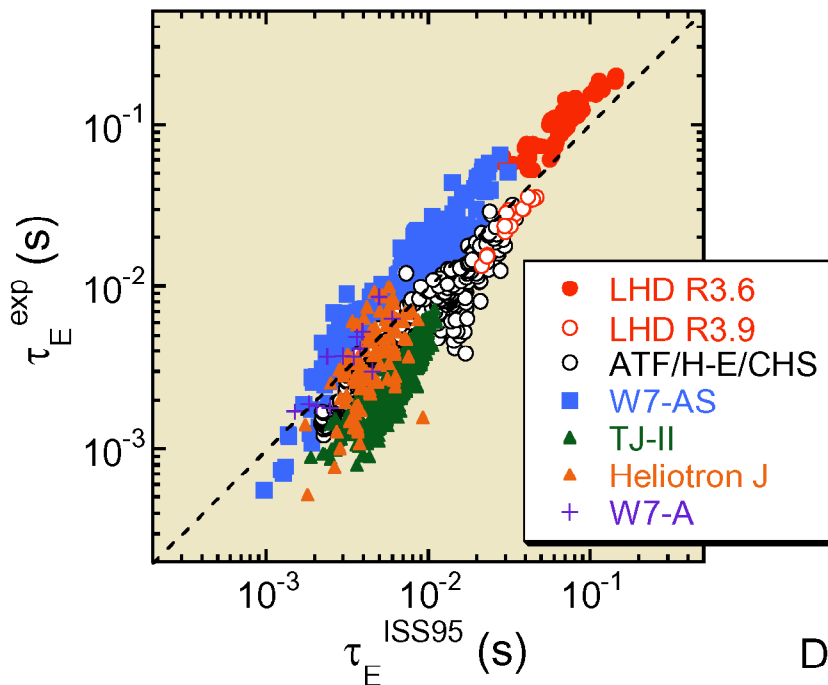
Under auspices of IEA Implementing Agreement
for Cooperation in Development of the Stellarator Concept



Originally, the activity was launched from the collaboration between ORNL(ATF) and IPP(W7-AS) , and then NIFS(CHS) and Heliotron E (Kyoto Univ.) joined.



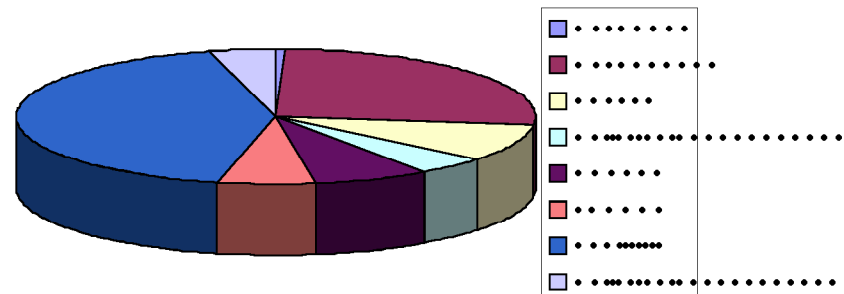
Derivation of international stellarator scaling 95 (ISS95) Nucl.Fusion (1996)
Renewal involving new data from new experiments and improved modes.
Reconsider a unified scaling law for energy confinement time.



$$\tau_E^{ISS95} = 0.079 a^{2.21} R^{0.65} P^{-0.59} \bar{n}_e^{-0.51} B^{0.83} t_{2/3}^{0.4}$$

$$\propto \tau_B \rho_*^{-0.71} \beta^{-0.16} v_*^{-0.04}$$

Addition of data from LHD, W7-AS, TJ-II and Heliotron J (HSX will join soon).
The presently available data : 2683 shots

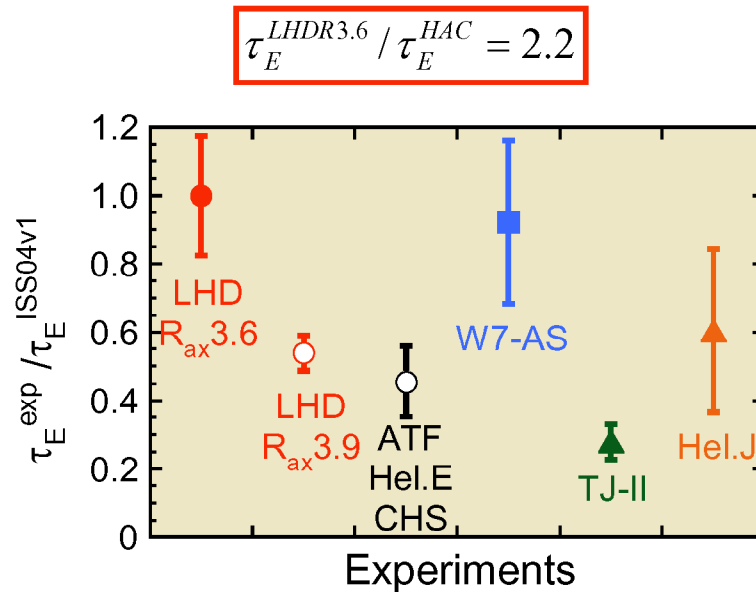
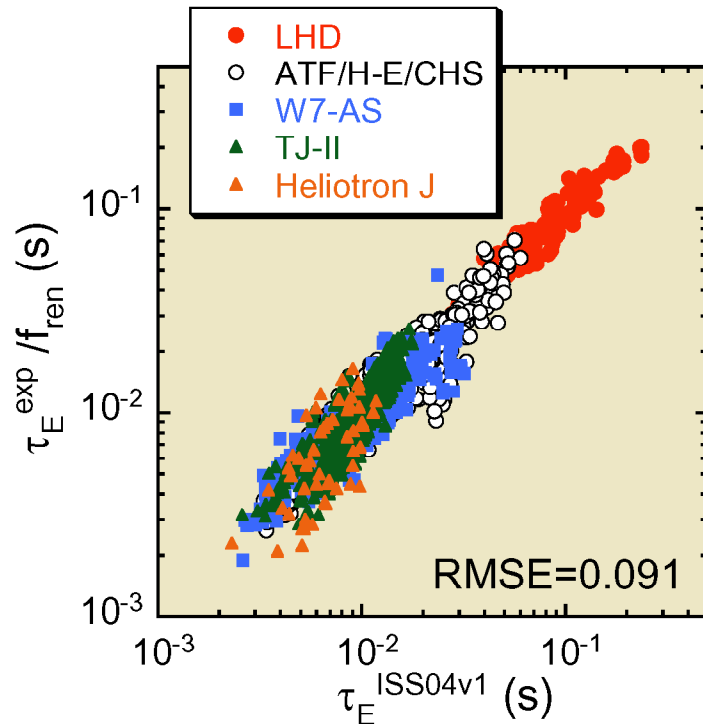


Database is jointly hosted by NIFS and IPP.

Unified scaling providing upper envelope of helical systems

Provisional

$$\tau_E^{ISS04v1} = 0.132 a^{2.32} R^{0.60} P^{-0.65} \bar{n}_e^{-0.59} B^{0.89} \tau_{2/3}^{0.41} \propto \tau_B \rho_*^{-1.09} \beta^{-0.25} v_*^{0.05} t^{1.24} \varepsilon^{0.27} a^{-0.35}$$



- Underlying physics of renormalization factors which contains uncertainties peculiar to each configuration.
 - ➔ Investigation of correlation of f_{ren} with physical parameters, ex. ε_{eff} .
- Employment of renormalization factor ➔ Can we derive size scaling?

There exist systematic gaps between each experiment.

1. W7-AS and heliotrons(ATF,H-E,CHS) : still unresolved

••Quite similar scaling expression from independent analysis

$$\begin{aligned} \tau_E^{HAC} &= 0.040 a^{2.06} R^{0.74} P^{-0.63} \bar{n}_e^{-0.53} B^{0.80} \tau_{2/3}^{0.39} \\ \tau_E^{W7AS} &= 0.115 a^{2.21} R^{0.74} P^{-0.54} \bar{n}_e^{-0.50} B^{0.73} \tau_{2/3}^{0.43} \end{aligned} \quad \left. \vphantom{\begin{aligned} \tau_E^{HAC} \\ \tau_E^{W7AS} \end{aligned}} \right\} \text{combined dataset does not give a reasonable result.}$$

Accept difference for magnetic configuration

→ Artificial parameter express difference between HT & W7-AS

→ ISS95 $\tau_E^{W7-AS} / \tau_E^{HAC} = 1.95$

2. Entire available data including LHD, TJ-II and Heliotron J

A simple regression analysis gives

$$\tau_E^{scl} = 0.30 a^{2.07} R^{1.02} P^{-0.60} \bar{n}_e^{-0.58} B^{1.08} \tau_{2/3}^{-0.16} \propto \tau_B \rho_*^{-1.95} \beta^{0.13} v_*^{-0.18} \tau^{-0.58} \varepsilon^{-1.49} a^{-0.55}$$

RMSE=0.101

••Dimensionally incorrect and strange expression.

••Contradict knowledge from each experiment, ex. gyro-Bohm, iota dependence.

Accept differences between configuration.

But configuration dependent parameter has not been clarified.

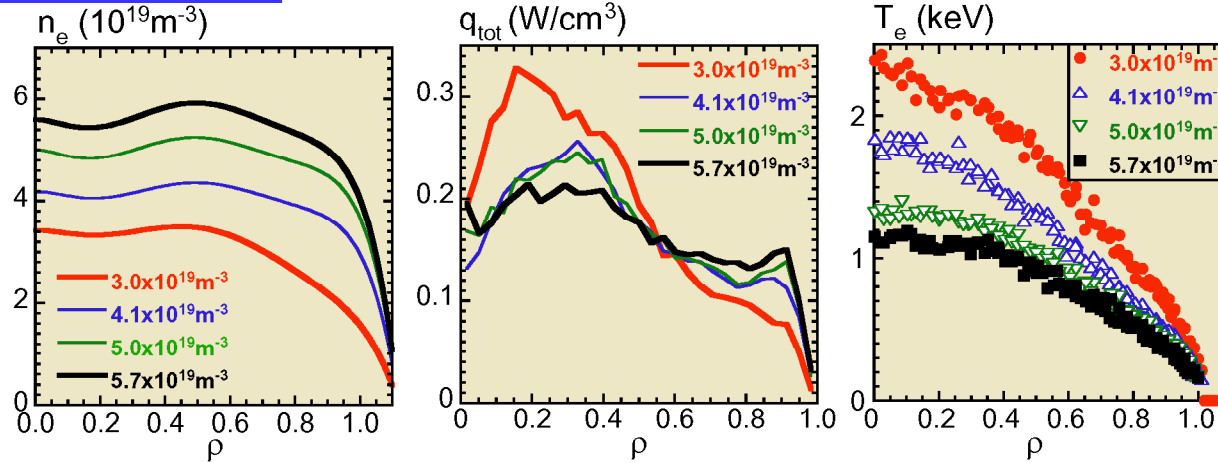
Renormalization on scaling gives a provisional unified expression.

$$f_{ren} = \langle \text{HISS95 of subset} \rangle / \langle \text{HISS95 of LHD with } R_{ax}=3.6\text{m} \rangle$$

Then regression analysis of τ_E^{exp} / f_{ren} and iteration of it.



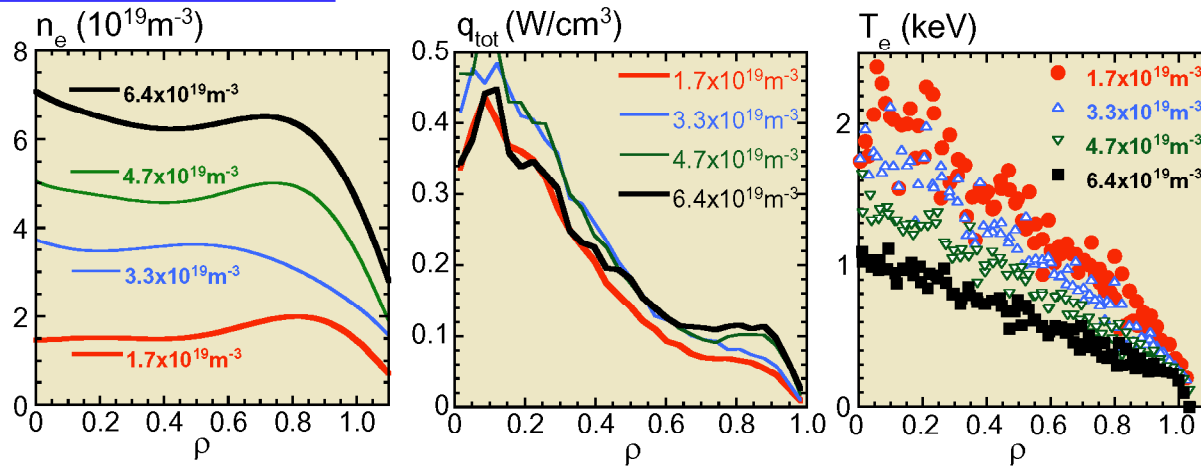
$R_{ax}=3.6m$, Saturation



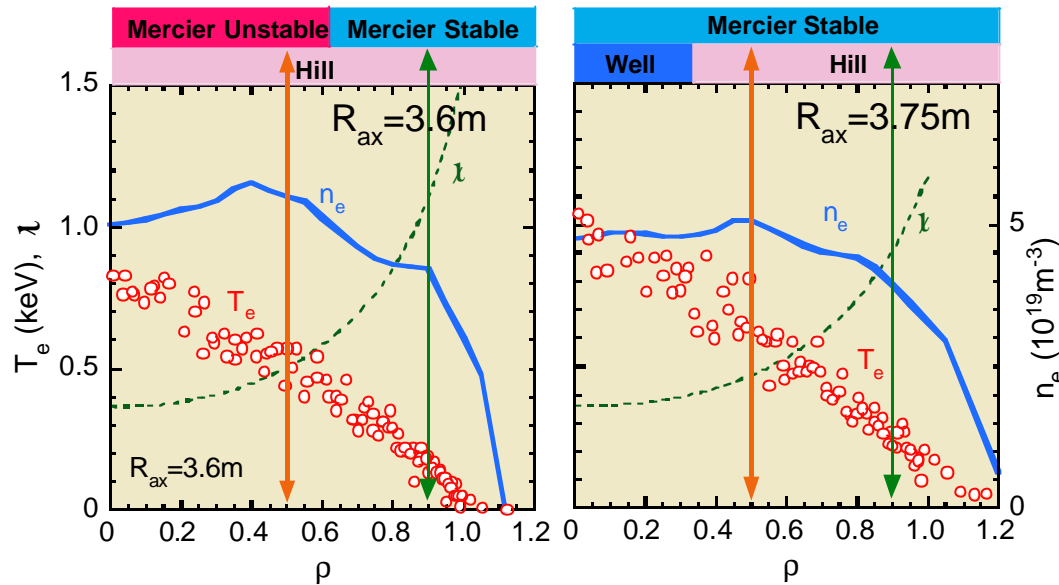
Off-axis beam arrangement & High density preventing beam penetration.

- Broadening heat deposition profile → Temperature follows it.
- Suggesting absence of profile resilience

$R_{ax}=3.75m$, No saturation

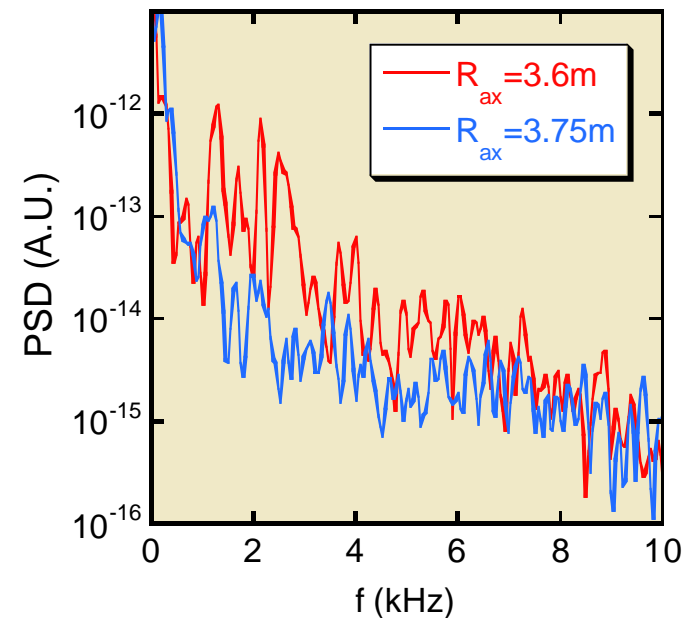


Dimensionally similar plasmas with different R_{ax}

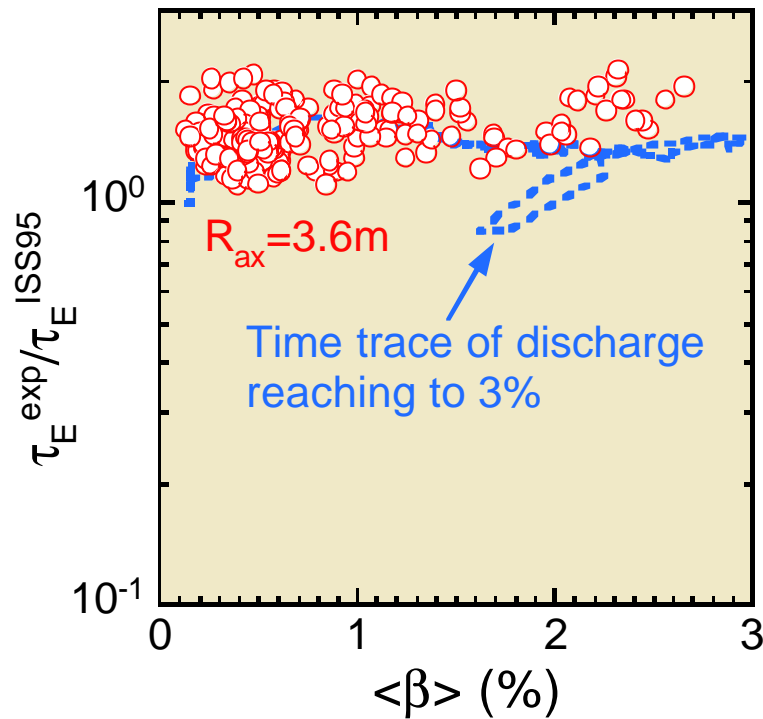


- Better heat transport in $R_{ax} = 3.6m$ in spite of unstable Mercier and larger fluctuation

R_{ax} (m)	3.6	3.75
Mercier($\rho=0.5$)	unstable	stable
P_{abs} (MW)	1.67	3.17
\tilde{B}/B_{eq}	1.75	0.50
ρ	0.5/0.9	
$-dp/d\rho$ ($10^4 J/m^3$)	1.6/1.9	1.7/1.8
χ_e (m^2/s)	1.4/1.0	2.4/1.8

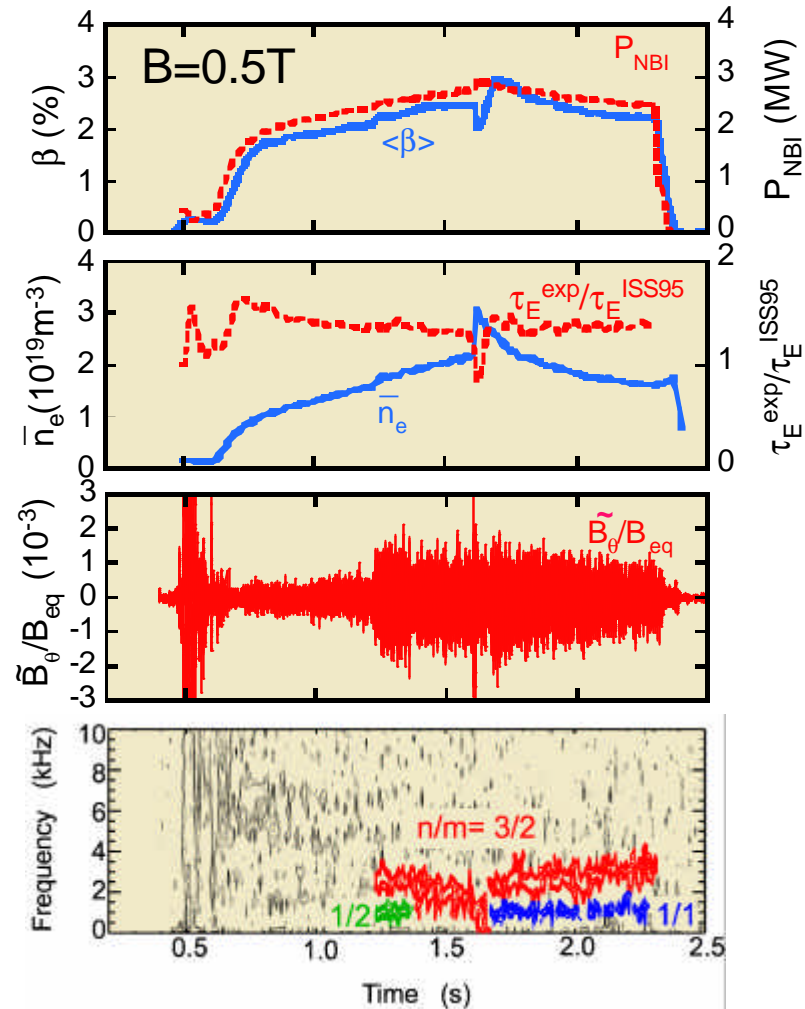


Favorable confinement at R_{ax} of 3.6m is maintained up to $\langle \beta \rangle$ of 3%



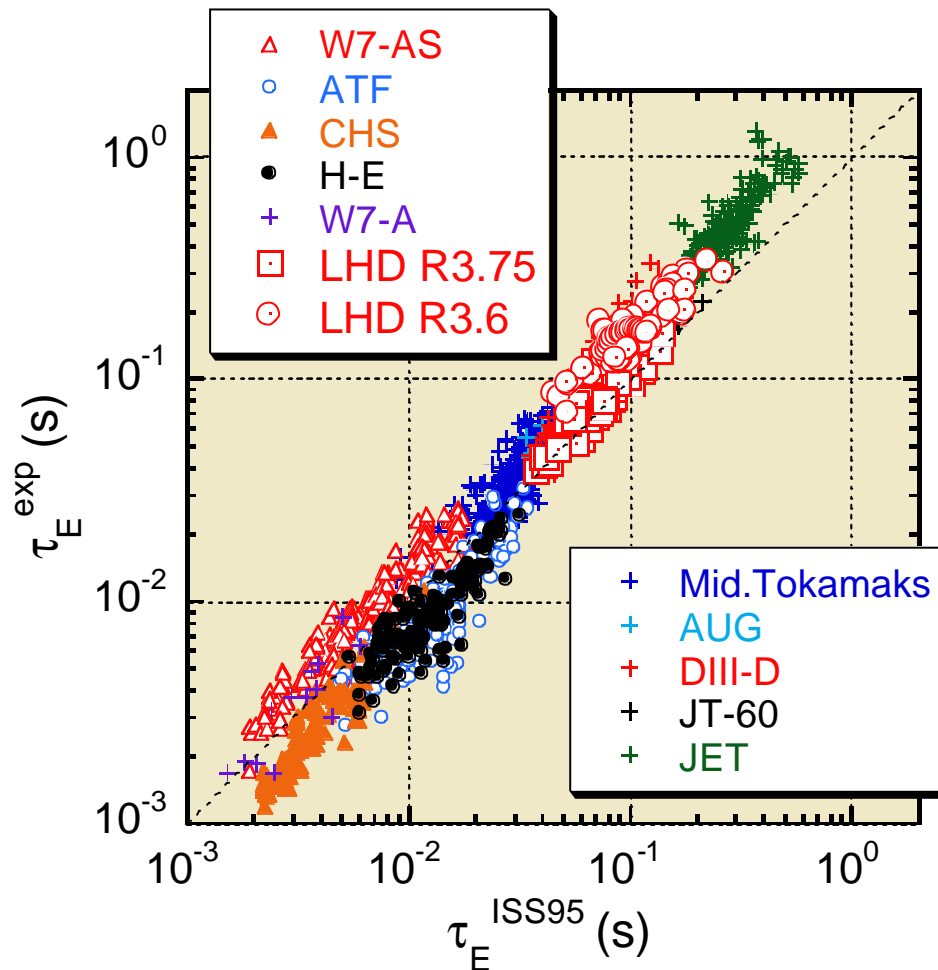
Confinement improvement over ISS95 $\tau_E^{exp}/\tau_E^{ISS95} \sim 1.5$ is robust at $R_{ax} = 3.6m$ for β .

Ü In spite of unfavorable MHD stability



\tilde{B}/B_{eq} reaches 0.1%

Global Energy Confinement Time



$$\tau_E^{ISS95} = 0.08 a^{2.21} R^{0.65} P^{-0.59} n_e^{-0.51} B^{0.80} t_{2/3}^{0.40}$$

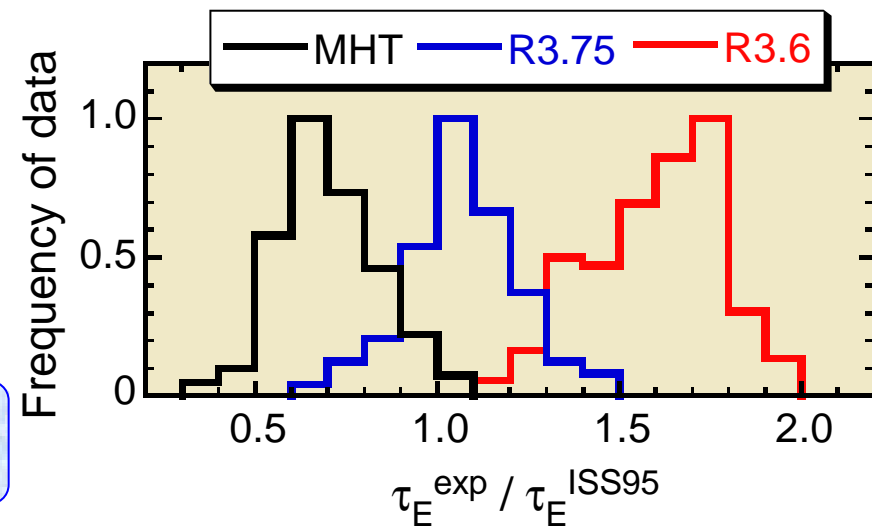
- Reference : *International Stellarator Scaling 95*
derived from medium-sized helical experiments

(ATF, Heliotron-E, CHS, W7-AS)

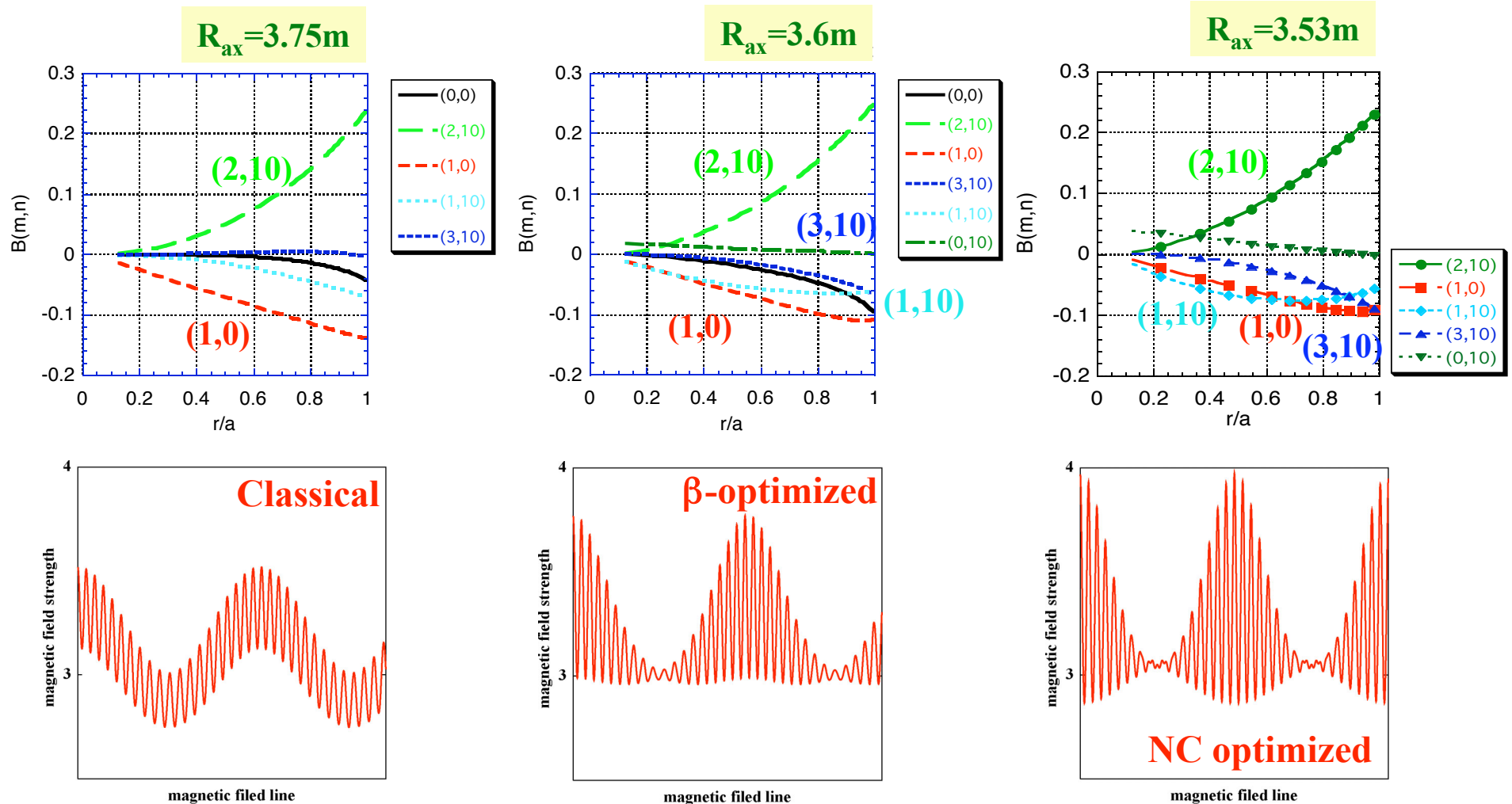
Near gyro-Bohm

$$t_E^{ISS95} \propto t_B r^{*-0.71} b^{-0.16} n^{*-0.04}$$

Similar to ITER ELMy-H scaling



Mod-B Profile of LHD Configurations



- ◆ Inward shift increases the mirror mode $(0,10)$, the sub-harmonic modes; $(1,10)$, $(3,10)$.



S. Murakami et al., Joint Meeting of US-Japan Workshop and Kyoto Univ. 21st COE Symposium, 3 March 2004



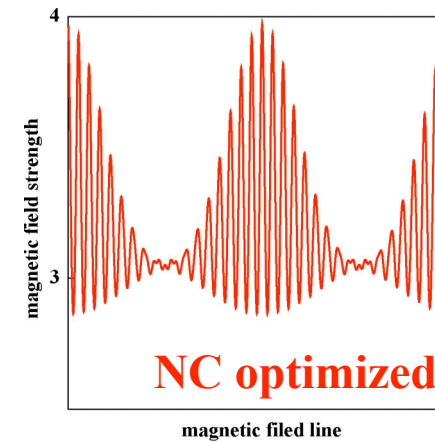
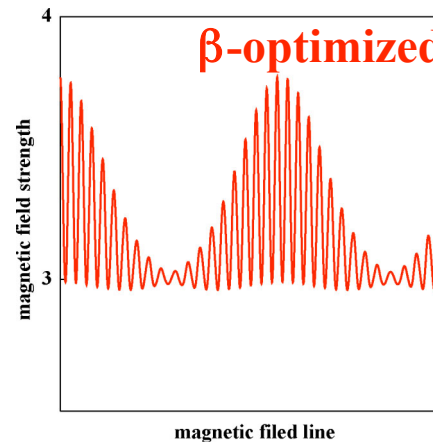
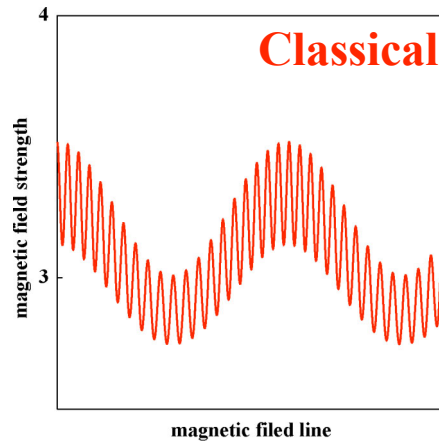
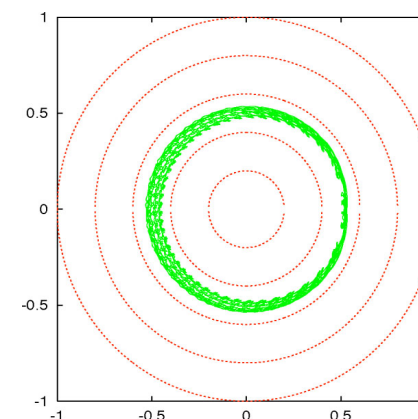
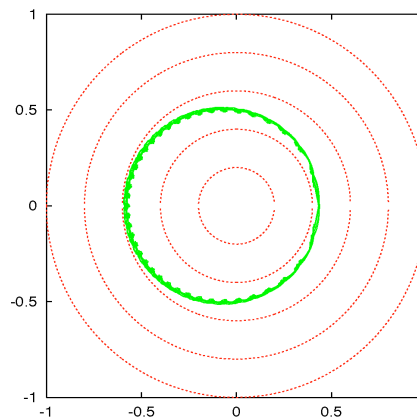
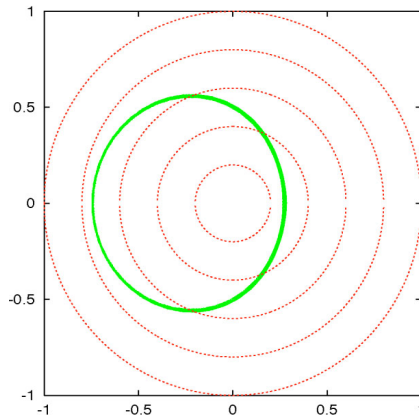
Trapped Particle Orbit

Toroidal
projection

$R_{ax}=3.75m$

$R_{ax}=3.6m$

$R_{ax}=3.53m$



$E=3.4MeV$
 $\beta_p=0.47\beta$
 $r_0=0.5a$
 $\beta_0=\beta/2$
 $\beta_0=0.0$

◆ Inward shift of R_{ax} improves the trapped particle orbit.



Basics – 1



Local ansatz allows an ordering of the linearized DKE $(r, \phi, \theta, \kappa, \mu)$

$$\frac{dr}{dt} \left\{ \frac{n'_0}{n_0} + \frac{q\Phi'}{kT} + \left(\frac{\kappa}{kT} - \frac{3}{2} \right) \frac{T'}{T} \right\} f_m + \frac{d\phi}{dt} \frac{\partial f_1}{\partial \phi} + \frac{d\theta}{dt} \frac{\partial f_1}{\partial \theta} = C_\mu(f_1)$$

in which **minor-radius** and **energy** coordinates appear only as parameters.

- 5D \longrightarrow 3D
- All neoclassical effects can be characterized by three *mono-energetic* transport coefficients Γ_{11} , Γ_{31} , Γ_{33} .

For benchmarking, it is sufficient to compare mono-energetic quantities of interest.

Monoenergetic Diffusion Coefficients

Matrix formulation of neoclassical transport is based on convolutions of monoenergetic coefficients.

- DKES: Drift Kinetic Equation Solver; uses moments representation of distribution function.

Low ν : need many moments to represent the boundary layer at the passing-trapped boundary.

- DCOM/MOCA follow drift-orbits of a sample population using Monte Carlo collision algorithm.

Low ν : need very long integration times to fully sample phase space; $\text{time} * \nu_{90} \sim 1$.

- MOCA used here because it can deal with very low collisionalities more easily than DKES.

- **Good benchmark agreement between DKES and orbit codes for wide range of ν and E_r .**

$$Q_j = D_{11} e^{-x} \frac{n}{n} \frac{Z_j e E_r}{T_j} + \left(x - \frac{3}{2} \right) \frac{T_j}{T_j} x^2 \sqrt{x} dx$$

Conventional matrix formulation needs only D_{11} for particle and heat transport, **but**

- **Sugama's correction for momentum non-conservation needs all three coefficients.**

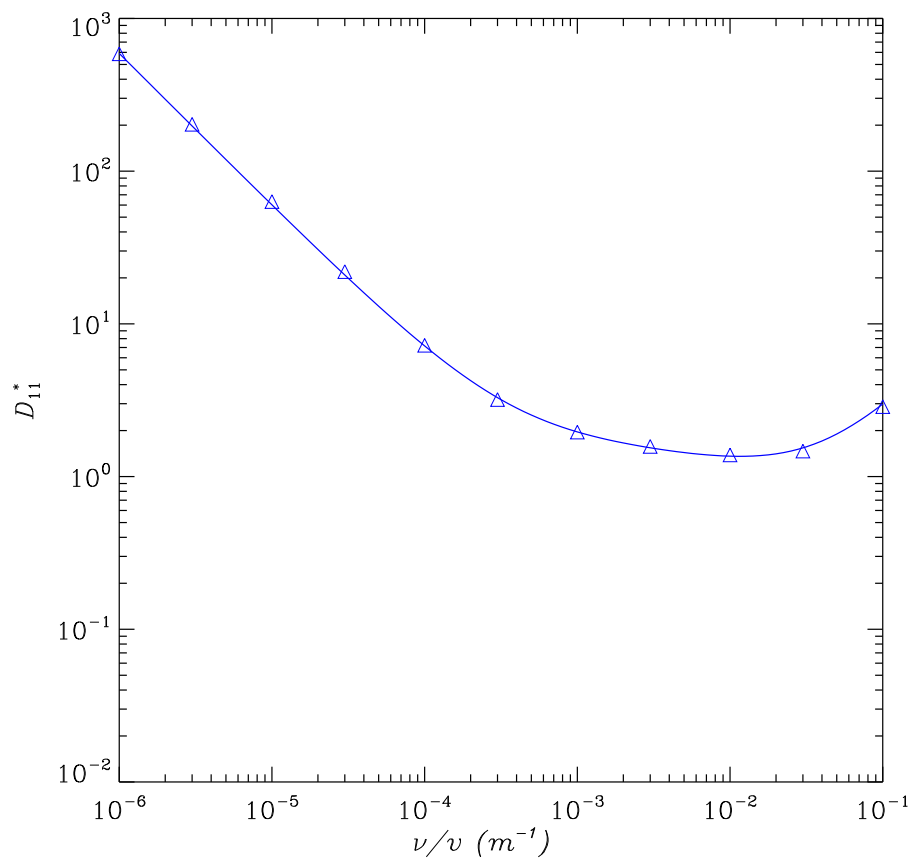
- D_{11} can be calculated by DKES or Monte Carlo orbit code; D_{33} and D_{31} come from DKES.

- D_{33} (conductivity) and D_{31} (bootstrap) have negligible dependence on E_r .

- **D_{11} is still the only computationally expensive part of the calculation.**

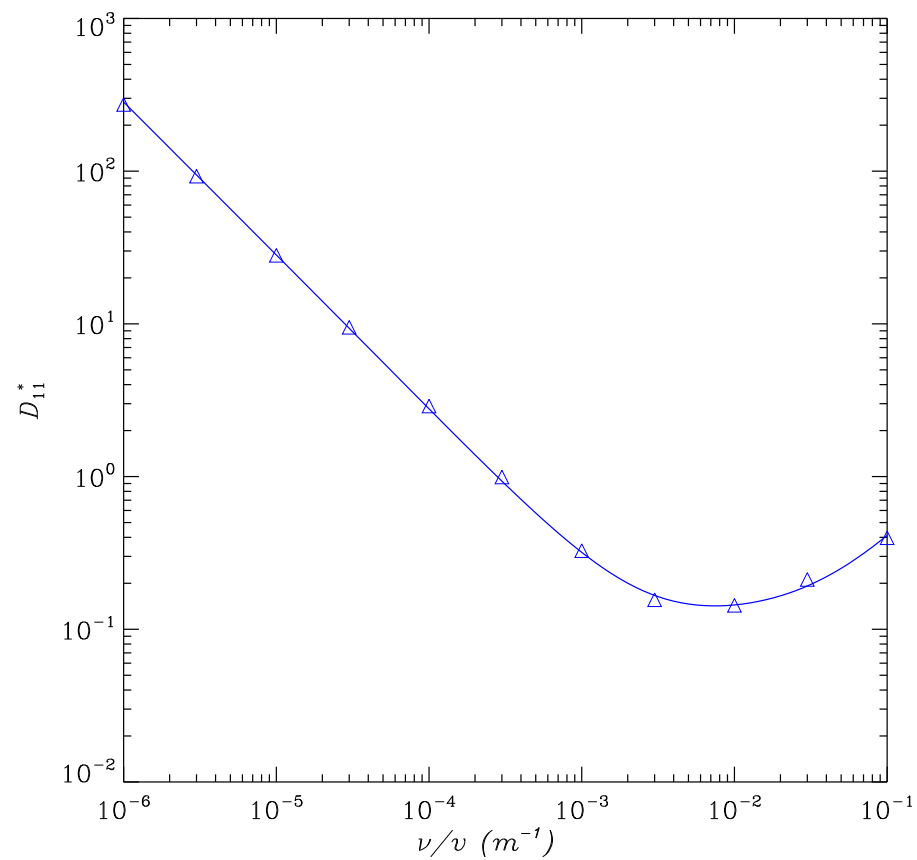
For more detail on the Sugama procedure see Don Spong's poster **RP1.023** (this session).

LHD Standard



$$\mathcal{A} = 0.1315 \quad \mathcal{B} = 1.82$$

W7X High Mirror



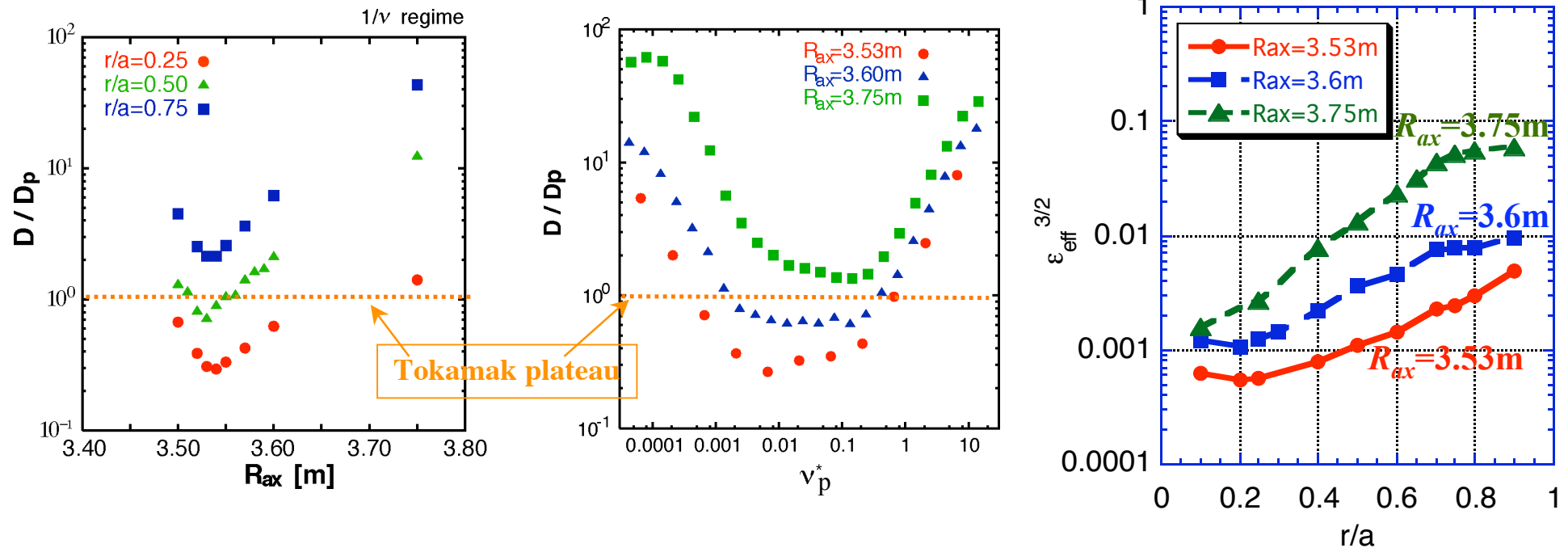
$$\mathcal{A} = -0.102 \quad \mathcal{B} = 50.4$$

Neoclassical Transport Optimized Configuration

Neoclassical transport analysis (by DCOM)

S. Murakami, et al., Nucl. Fusion 42 (2002) L19.

A. Wakasa, et al., J. Plasma Fusion Res. SERIES, Vol. 4, (2001) 408.



- ◆ We evaluate the neoclassical transport in inward shifted configurations by **DCOM**.
- ◆ The optimum configuration at the $1/\beta$ regime $\Rightarrow R_{ax} = 3.53\text{m}$.
($\beta_{eff} < 2\%$ inside $r/a = 0.8$)
- ◆ A strong inward shift of R_{ax} can diminish the NT to a level typical of so-called "advanced stellarators".

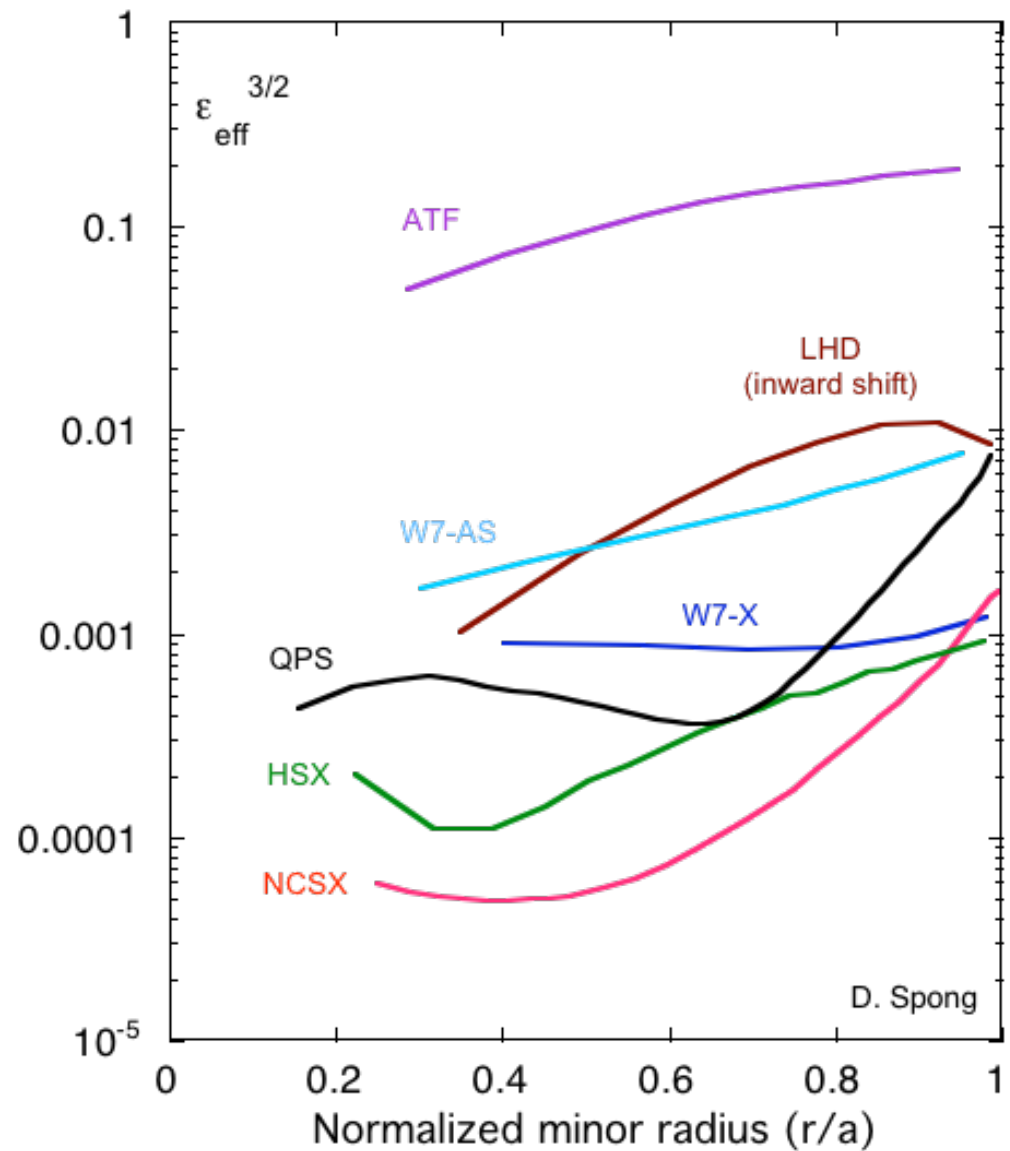


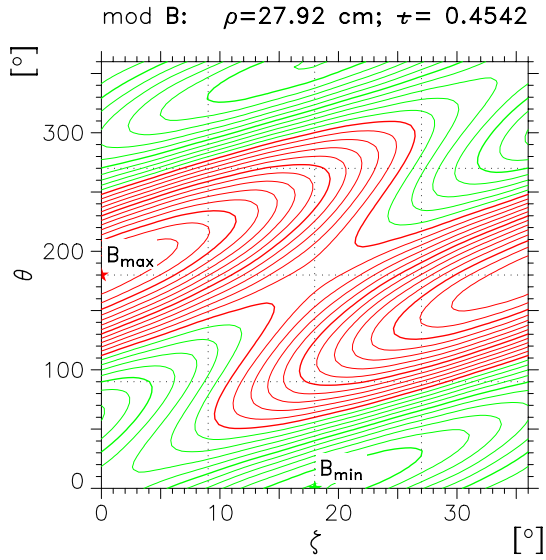
S. Murakami et al., Joint Meeting of US-Japan Workshop and Kyoto Univ. 21st COE Symposium, 3 March 2004



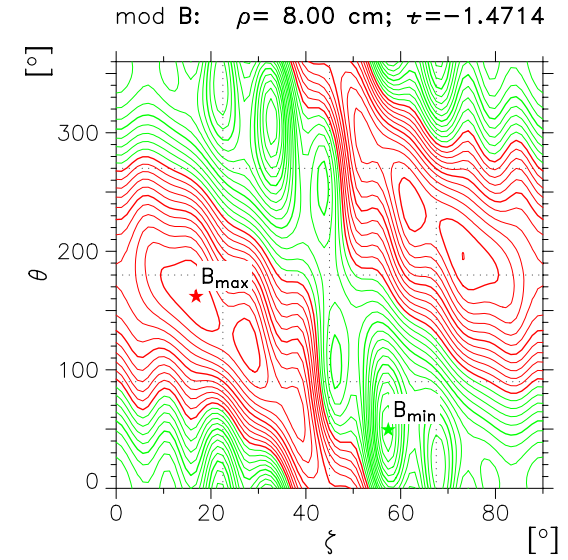
Quasi-Axisymmetric: Very Low effective ripple

- Very low effective helical ripple
 $\epsilon_{\text{eff}} \sim 1.4\%$ at edge
 $\sim 0.1\%$ in core
- Produces low flow-damping to allow manipulation of flows for flow-shear stabilization, control of E_r
- Allows balanced-NBI
24% loss at 1.2T, drops as B rises
- ϵ_{eff} calculated by NEO code (Nemov & Kernbichler)

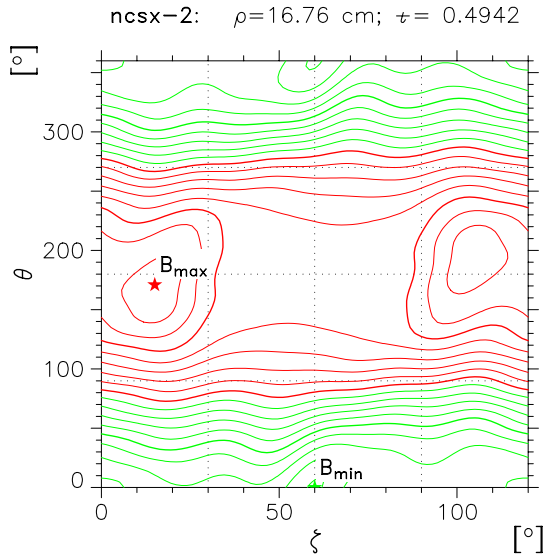




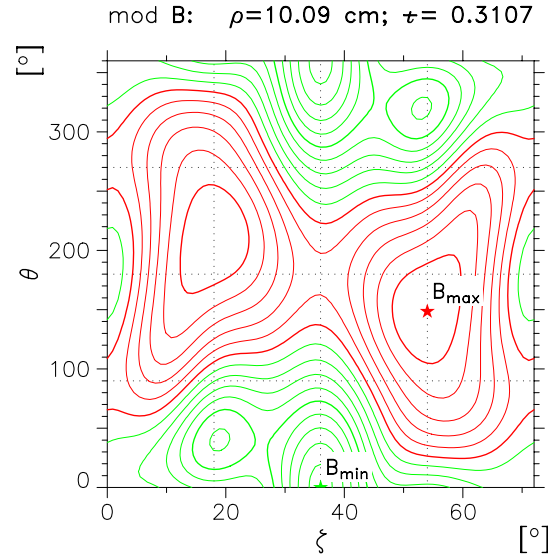
no. of Fourier coefficients for mod B: 12
 increment of mod B values: .01
 $B_{\max} / B_0 = 1.130$ $B_{\min} / B_0 = .889$
 av. $\epsilon_h = 5.21\%$, trapped part. $\langle f_t \rangle = .483$



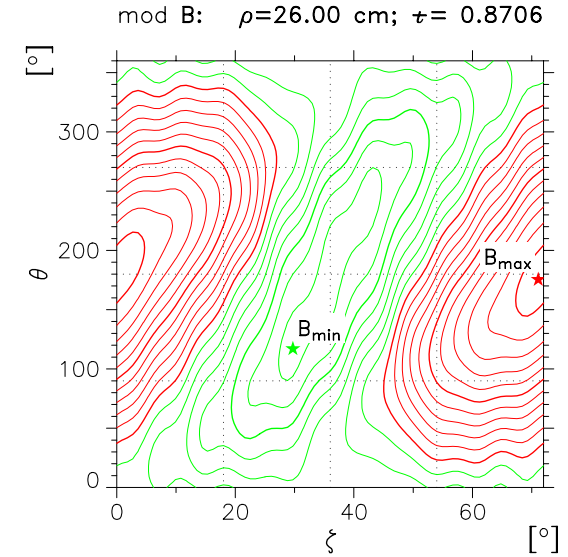
no. of Fourier coefficients for mod B: 38
 increment of mod B values: .01
 $B_{\max} / B_0 = 1.110$ $B_{\min} / B_0 = .852$
 av. $\epsilon_h = 6.75\%$, trapped part. $\langle f_t \rangle = .449$



no. of Fourier coefficients for mod B: 33
 increment of mod B values: .01
 $B_{\max} / B_0 = 1.076$ $B_{\min} / B_0 = .909$
 av. $\epsilon_h = 1.16\%$, trapped part. $\langle f_t \rangle = .383$



no. of Fourier coefficients for mod B: 23
 increment of mod B values: .01
 $B_{\max} / B_0 = 1.060$ $B_{\min} / B_0 = .906$
 av. $\epsilon_h = 3.41\%$, trapped part. $\langle f_t \rangle = .344$



no. of Fourier coefficients for mod B: 31
 increment of mod B values: .01
 $B_{\max} / B_0 = 1.105$ $B_{\min} / B_0 = .926$
 av. $\epsilon_h = 5.71\%$, trapped part. $\langle f_t \rangle = .443$

Stellarator Transport from a Tokamak Perspective

One fundamental difference in neoclassical transport:

particle transport is not intrinsically ambipolar; cause is lack of symmetry
unequal radial currents lead to charge-up and finite E_r .
ion and electron fluxes depend differently on E_r , so net radial current varies with E_r .
 E_r stops changing when balanced fluxes are achieved: **this is the ‘ambipolar’ E_r** .

There are two commonly occurring solutions (roots) to $\Gamma_e = \Gamma_i$:

Ion root: ions *were* leaving faster than electrons, so $E_r < 0$

Ion flux is suppressed by ExB de-trapping from local ripple wells.

Ion flux is **much lower** than $E_r=0$ flux.

Electron root: electrons *were* leaving faster than ions, so $E_r > 0$

electron root was relatively rare – most often seen with high T_e ECH.

Second fundamental difference is **local magnetic-well trapping**:

In the ion root, electrons are typically in the ‘ $1/\Omega$ regime’:

fewer collisions lead to longer radial drift of locally trapped particles.

electron flux depends strongly on T_e : $\Gamma_e \sim T_e^{3.5}$; $Q \sim T_e^{4.5}$.

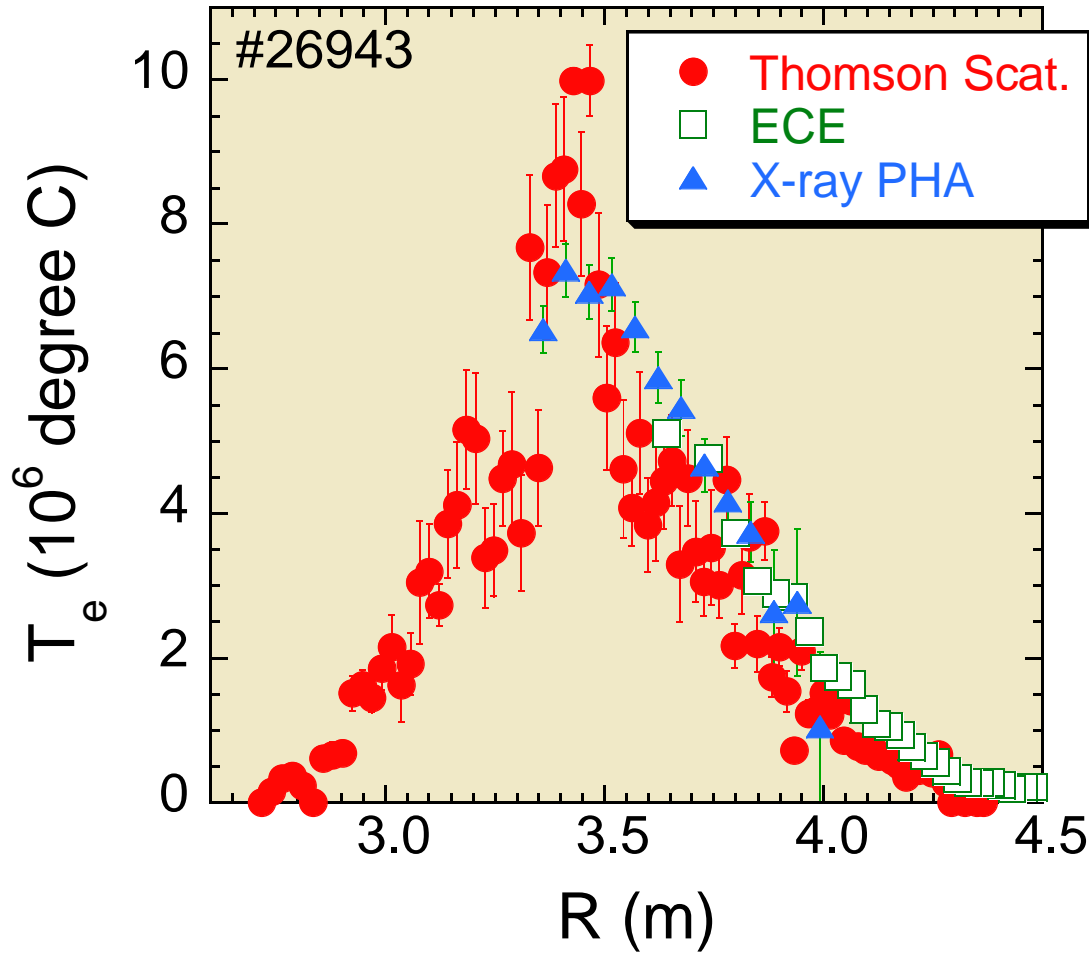
ambipolarity forces the ion flux to match the electron flux.

Fluxes are proportional to ‘**effective ripple**’, which is low in ‘optimized’ stellarators.

NCSX has very low effective ripple, but it can be raised by at least a factor of 5.



Electron temperature has reached 10 keV



Achieved parameters

$T_e(0)$ 10 keV

$T_i(0)$ 2 keV

$\langle n_e \rangle$ $5 \times 10^{18} \text{ m}^{-3}$

τ_E 0.05 s

Discharge duration 0.4s

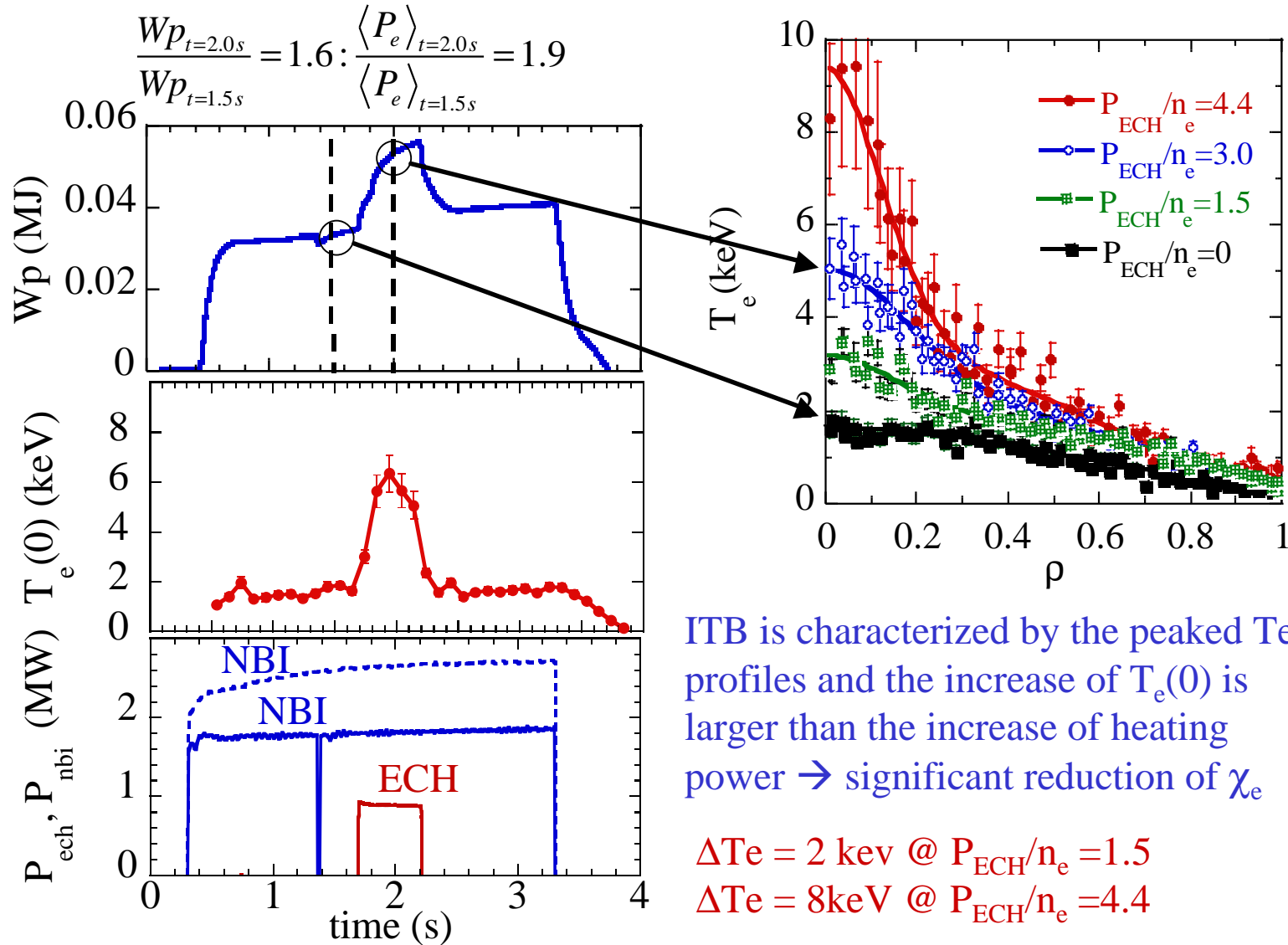
Experimental conditions

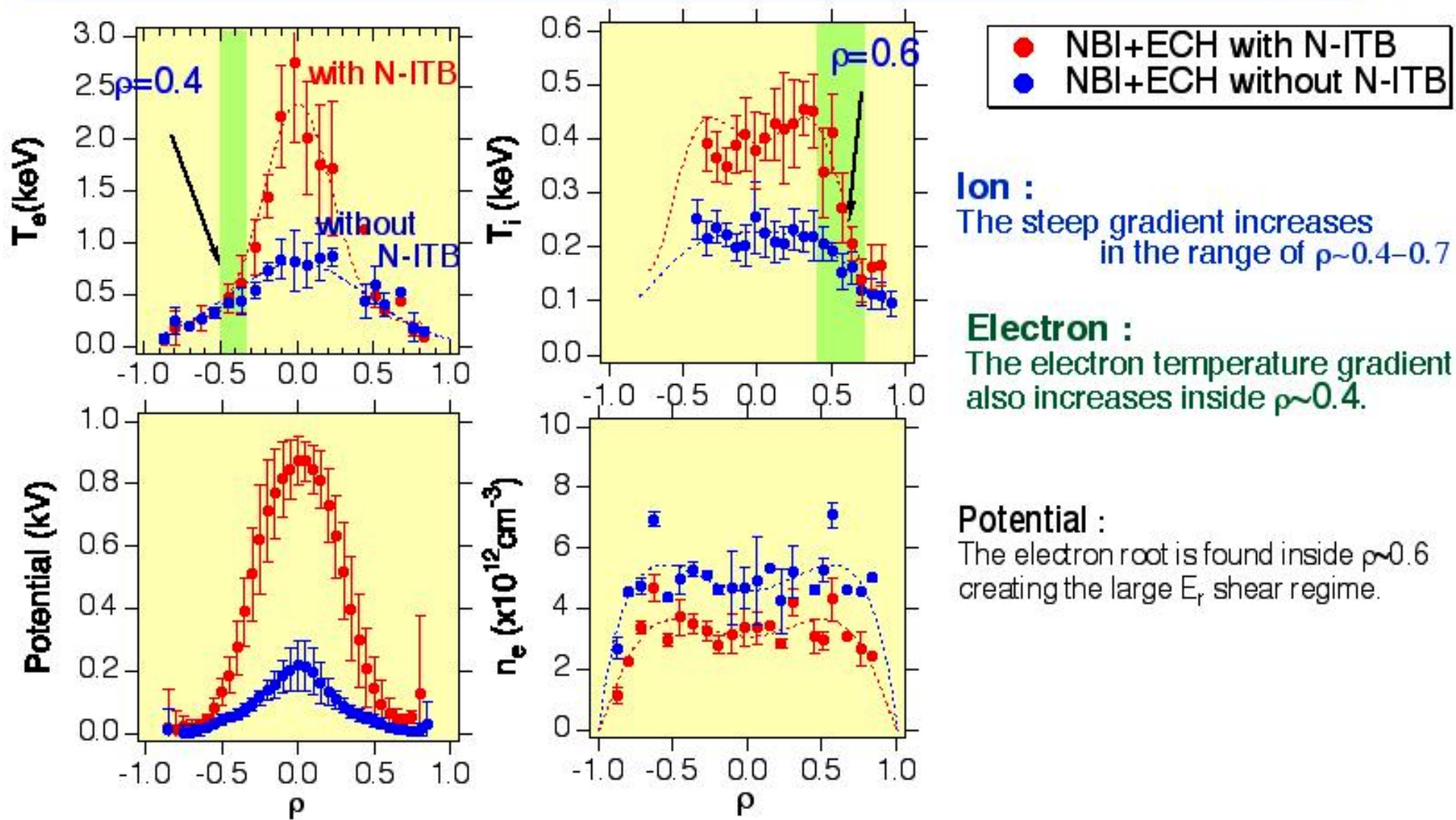
ECRH 1.2 MW

B 2.976 T

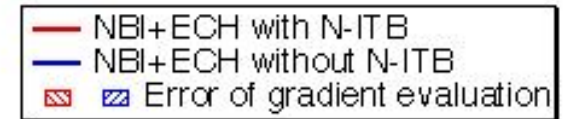
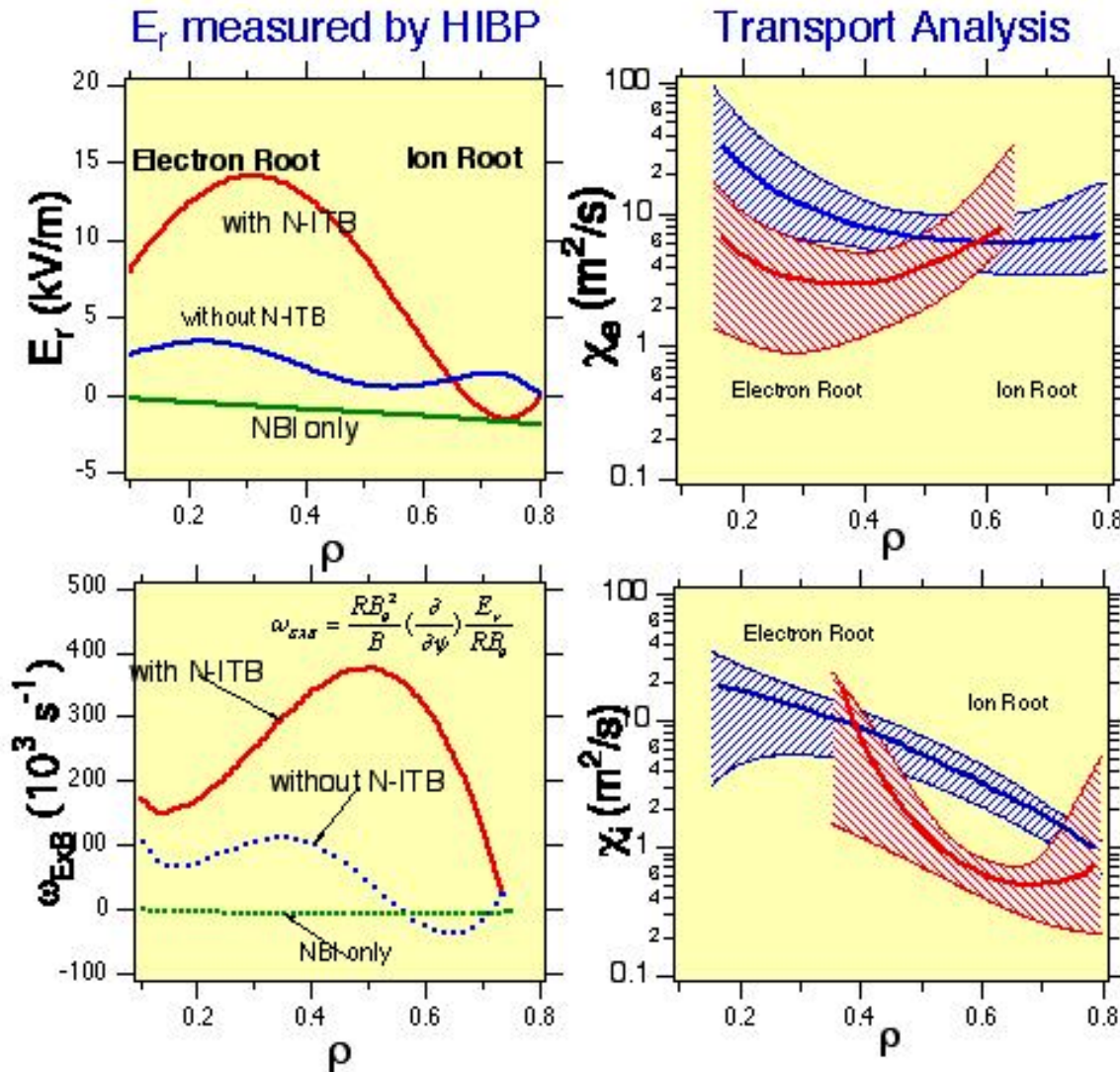
R_{ax} 3.5 m

Electron temperature profiles of ITB plasma in LHD





Steep T_i gradient is found in E_r shear regime.



- $E_r \sim 15 \text{ kV/m}$ with N-ITB
- $E_r < 5 \text{ kV/m}$ without N-ITB
- Small negative E_r without ECH

- $\omega_{E \times B} \sim 4 \times 10^5 \text{ s}^{-1}$,
 $dE_r/dr \sim 300 \text{ kV/m}^2$ with N-ITB
- $\omega_{E \times B} \sim 1 \times 10^5 \text{ s}^{-1}$ without N-ITB

The N-ITB plasma gives reduced χ_e at $\rho \sim 0.4$ compared to plasma without N-ITB

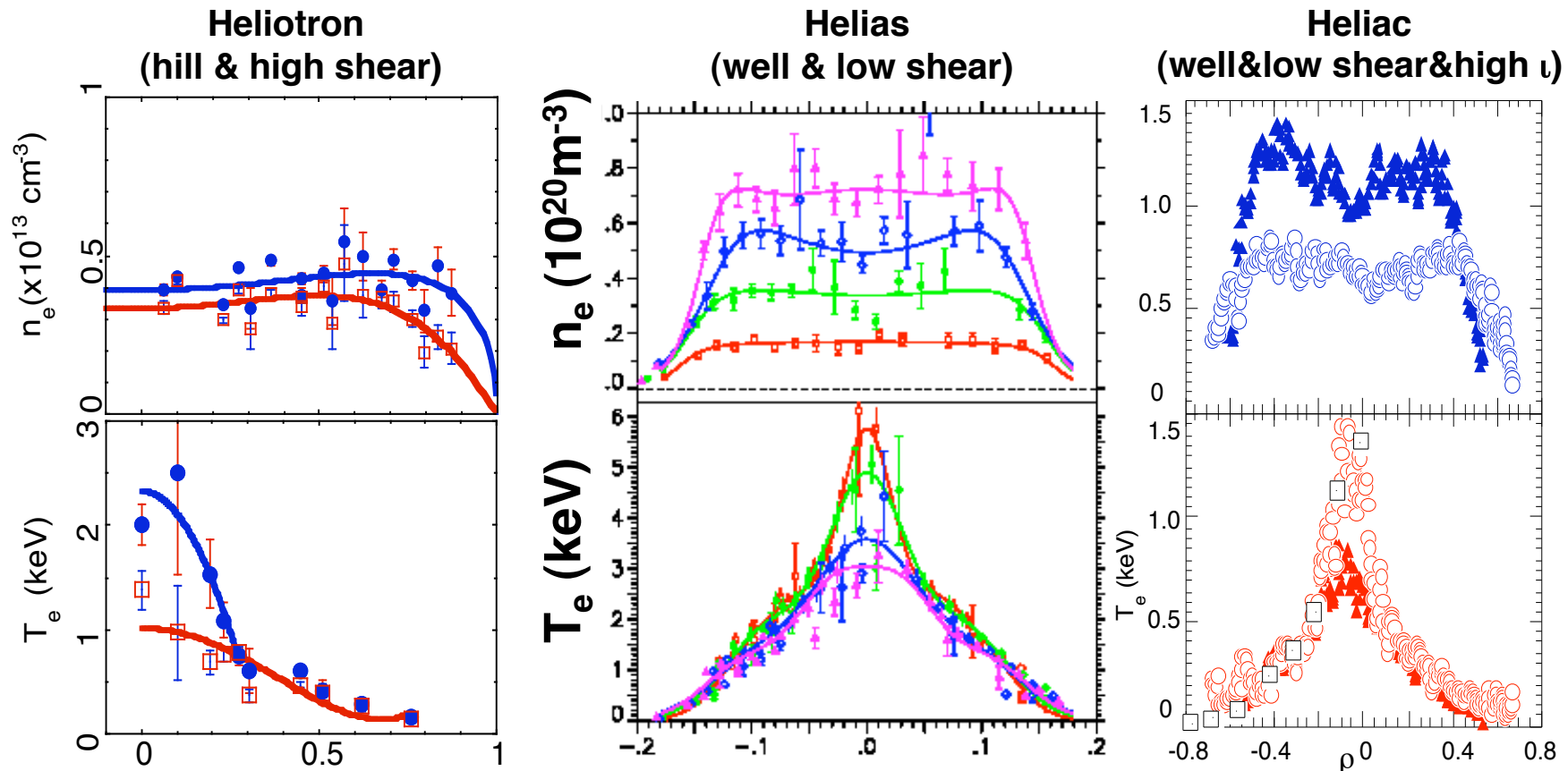
The present transport analysis shows the χ_i reduction at $\rho \sim 0.6$ for N-ITB plasma.

Difference between transport properties of ion and electron is to be studied in future.

ITBs in stellarators

Regardless of configuration, ITBs in stellarators show a common feature.

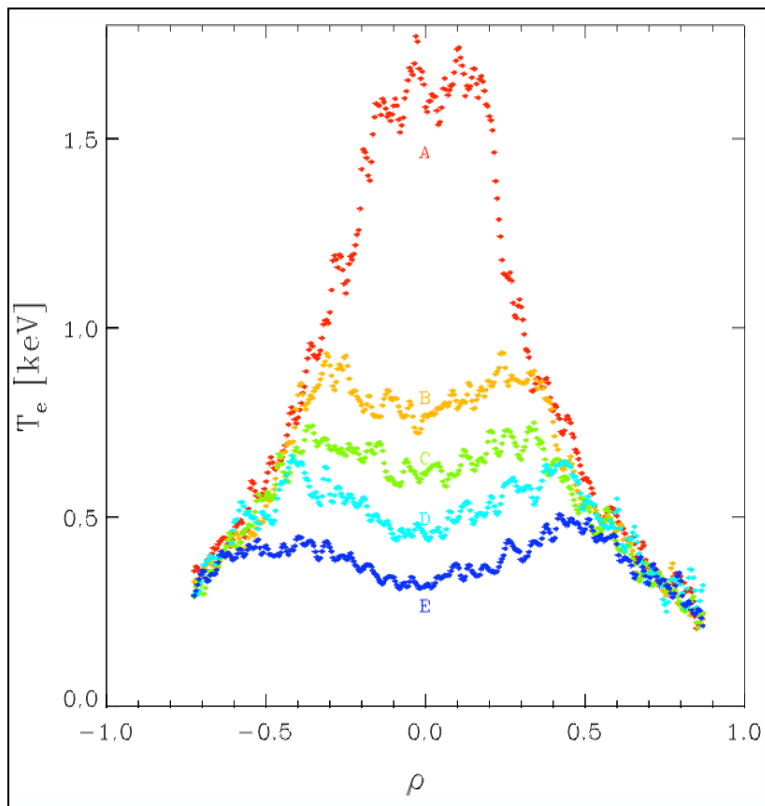
In ECR-heated discharges



In low density regimes, the bifurcation occurs and ITB can be created.

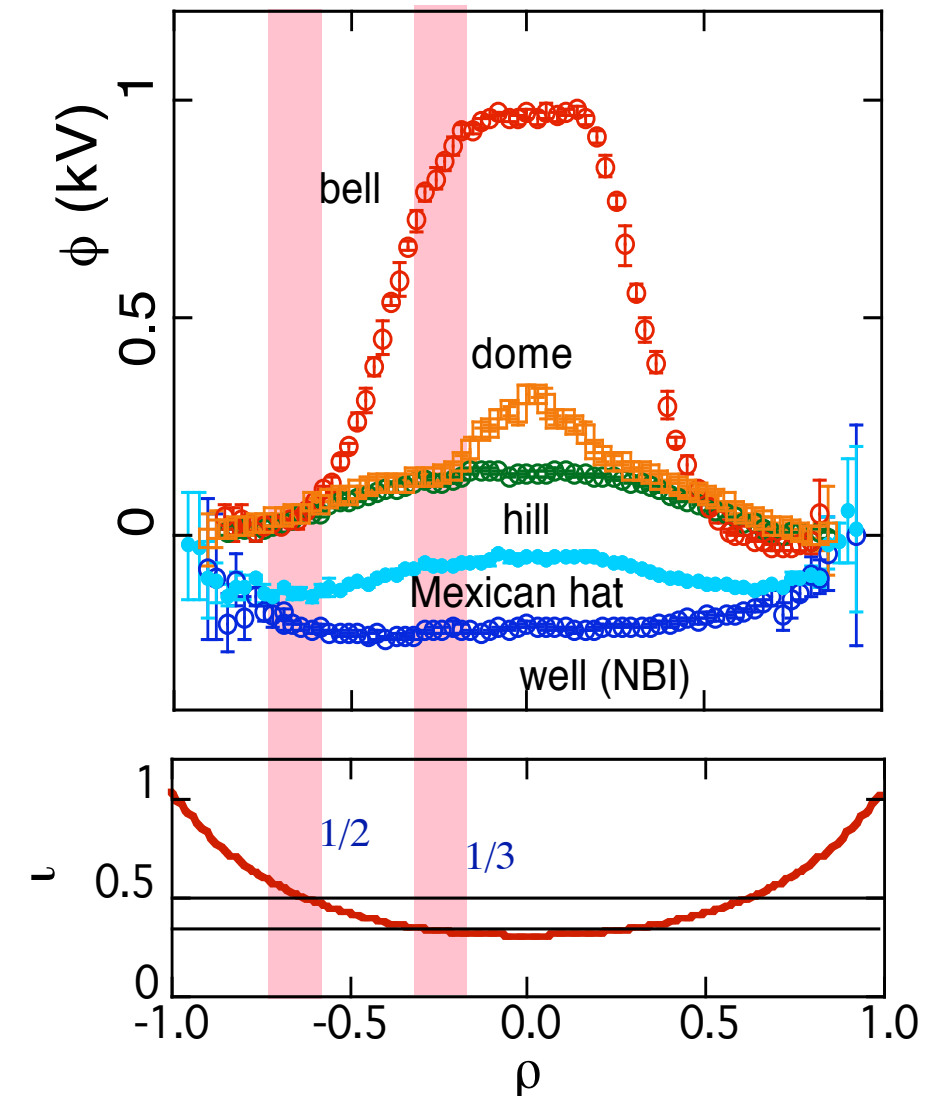
Rational Surface as Barrier

Rational surface as transport barrier



N. Lopes Cardozo et al., *PPCF* **39** B303(1997)

Q-comb model reproduces the profiles.
(reduction in χ at rational surfaces)



Rational surface is a key to determine the barrier position?

Generalizations about Stellarator Transport

Neoclassical transport is dominant in many stellarator plasmas;
those with $T_e(0) > 2$ keV – typically all ECH discharges have strong neo transport.

Cold plasmas - **high density** - have insignificant neoclassical transport.
Includes H* and HDH modes in W7-AS: highest confinement regimes!

LHD plasmas have large anomalous transport for $R_{axis} \leq 3.75$ m
Reduced neoclassical transport is not the cause of higher β_E !

The cause of anomalous transport is very poorly understood.
It might be the same kinds of microturbulence as in tokamaks.
There are no broadly established anomalous ‘transport models’.

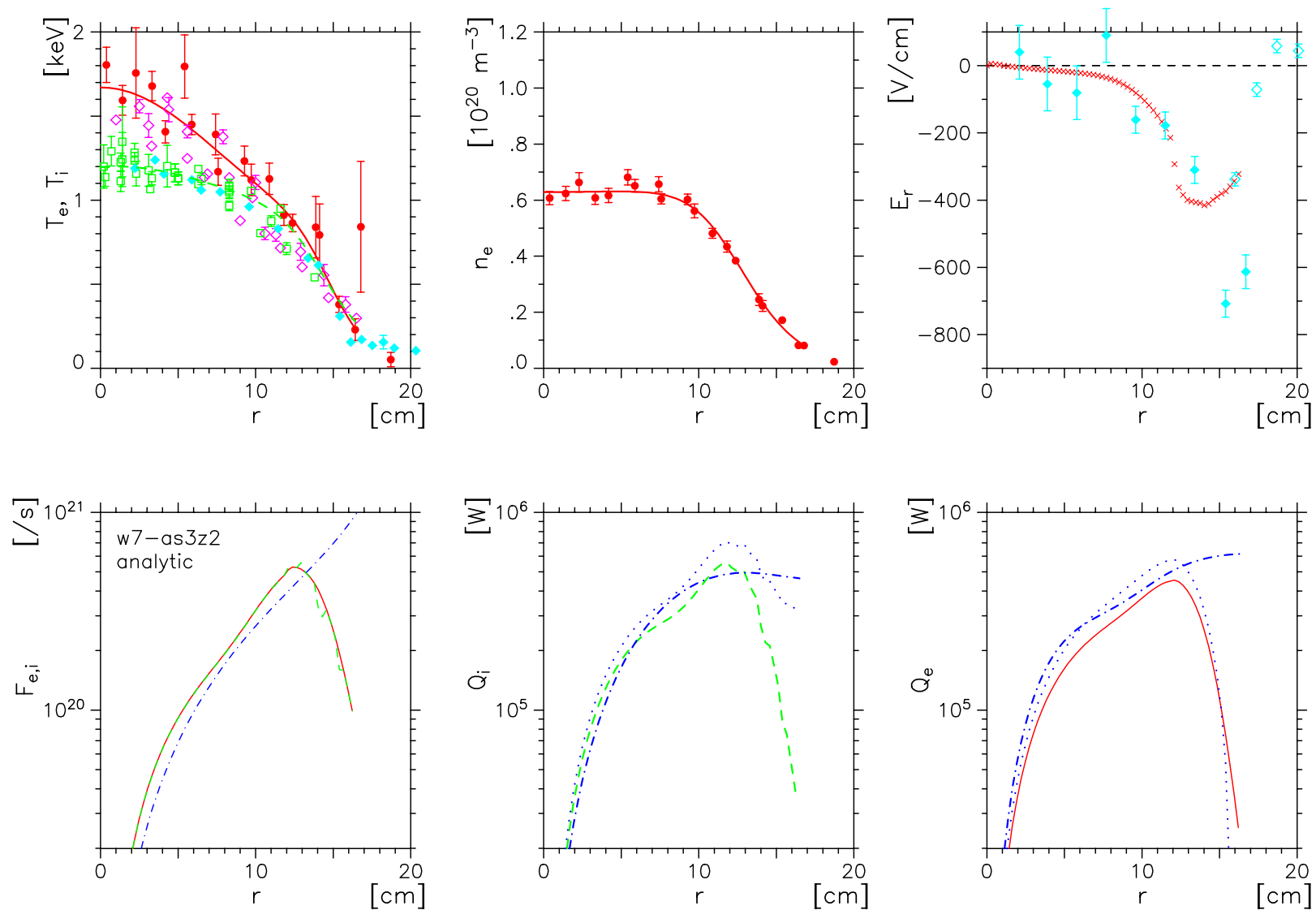
Radiation is important in **high density** stellarator plasmas.
impurities are not fully stripped at these low T_e , so they radiate strongly.
Impurity accumulation is observed in some regimes, but it is not understood.

Rotation is typically rather small because the helical viscosity is strong.

H-modes and ITBs are observed – but the causes may be different in stellarators.

Ohmic heating ~ 0 , so off-axis heating produces centrally flattened $T_e(r)$
no ‘profile consistency’ is observed in these cases.

shot 34313: 680 kW NBI, 750 kW ECRH absorbed power



neoclassical **ion** and **electron** fluxes compared to
fluxes from **particle and energy balance**



WENDELSTEIN 7-AS

The High Density H-Mode

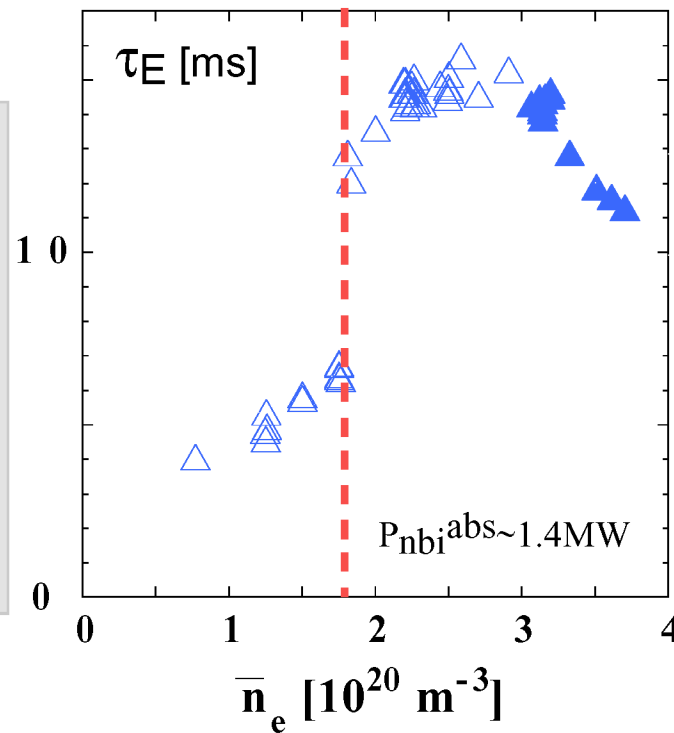
IPP

The HDH-Mode is a High Performance ELM-free H-Mode
It has enabled high-density island-divertor studies.

NC->HDH

Normal Confinement (NC)

High Density H-Mode (HDH)



at high n_e

- poor density control
- impurity accumulation
- Prad in center
- > radiation collapse
- > transient

$$\bar{n}_{e,\text{max}} \sim 2.5 \cdot 10^{20} \text{ m}^{-3}$$

above n_e^{thr}

- good density control
- no impurity accumulation
- high Prad at edge
- high energy confinement
- quasi-stationary

$$\bar{n}_{e,\text{max}} \sim 4 \cdot 10^{20} \text{ m}^{-3}$$

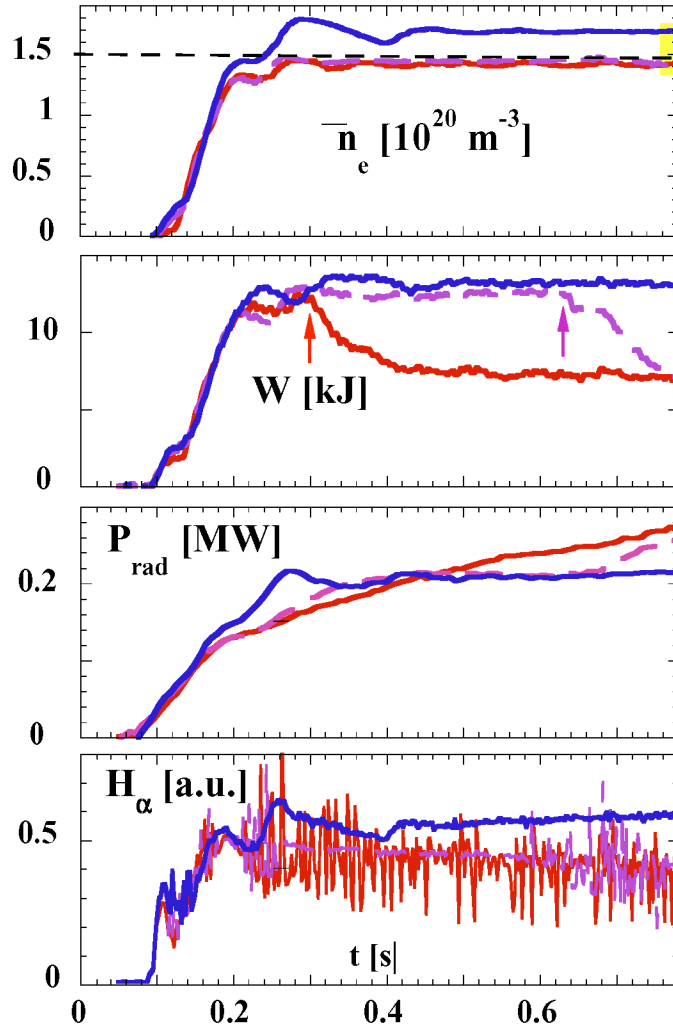


WENDELSTEIN 7-AS

Global Behavior: near HDH - NC transition density



NC->HDH



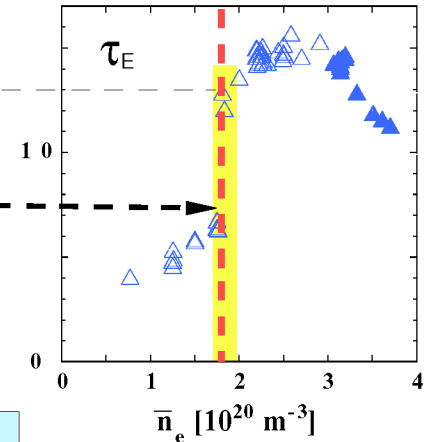
As the density threshold is approached:

~2x increase in stored energy

● The phase of high confinement becomes longer.

● Radiation remains stationary longer.

● ELMing decreases.



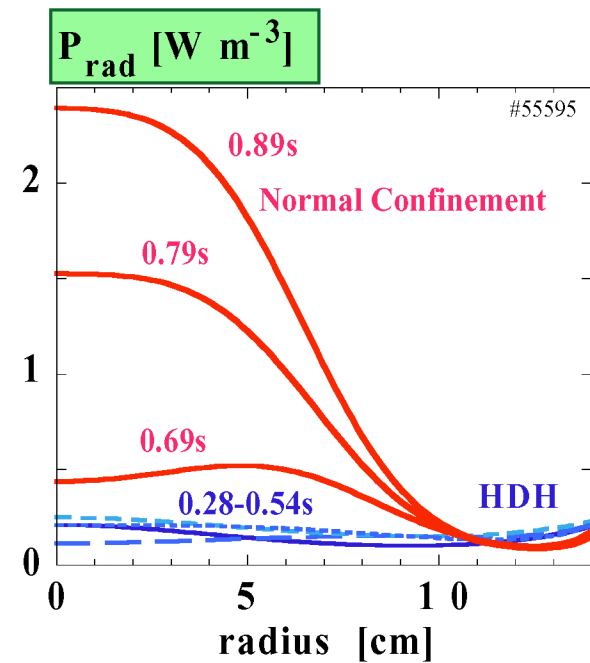
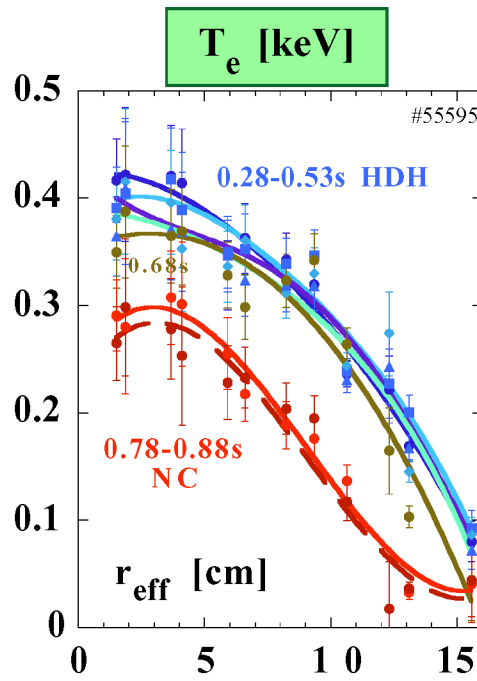
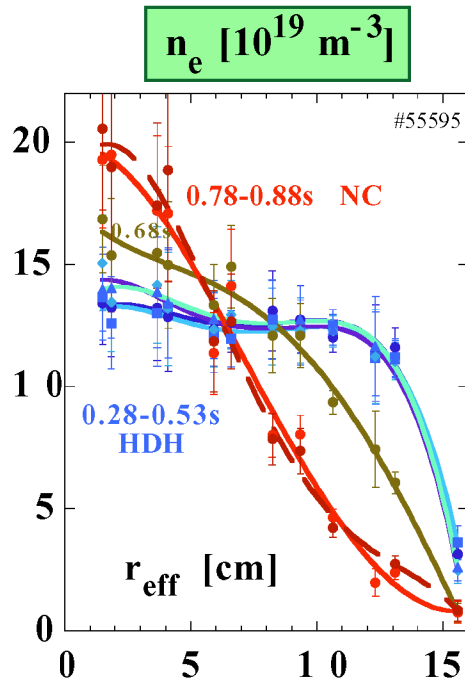


Profile Development



$n_e(r)$: Normal Confinement is Peaked, HDH is Flat

Density, Temperature & Radiation Profiles



	$n_e(r)$	$T_e(r)$	$P_{rad}(r)$
NC	peaked	peaked	peaked, increasing
HDH	broad	peaked	hollow, stationary

NC vs. HDH

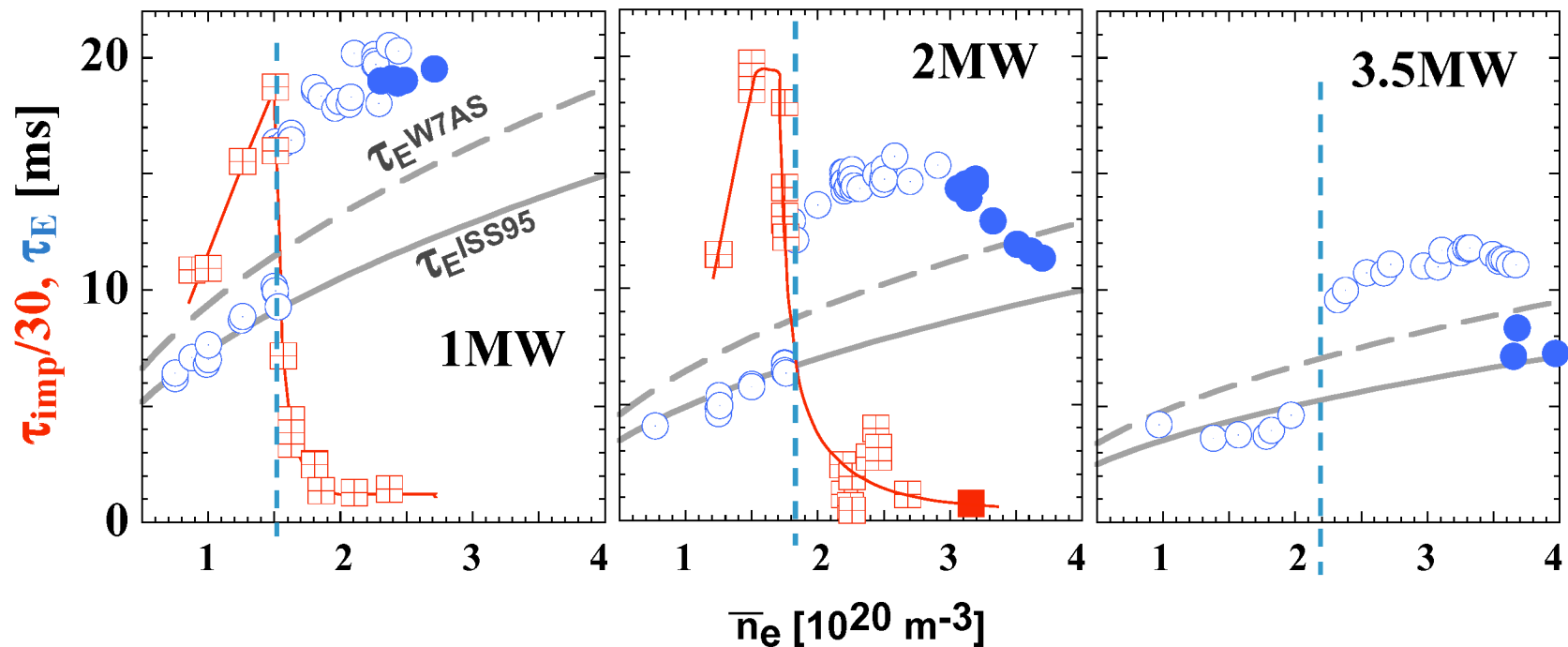


WENDELSTEIN 7-AS

HDH Exists over a Wide Range of P_{nbi} & Density

τ_E and τ_{AI} vs. n_e (quasi-stationary discharges)

IPP



- The NC→HDH transition density increases with P_{nbi}
- τ_E increases sharply at the transition
- τ_{imp} decreases sharply at the transition, approaching τ_E at higher n_e
- τ_E is higher than conventional scalings in HDH-Mode

NC→HDH



WENDELSTEIN 7-AS

SUMMARY

- of basic HDH features -

The Wendelstein 7-AS High Density H-Mode is an ELM-free H-mode

- has broad, flat n_e -profiles with a steep n_e -gradient at edge
- has parabolic-like T_e -profiles
- collisionality: impurities in Pfirsch-Schlüter-, background plasma in plateau-regime

- with low impurity and high energy confinement times
- allows steady-state operation [stationary $n_e(t)$ and $P_{\text{rad}}(t)$] for $n_e \leq 4 \cdot 10^{20}/\text{m}^3$
- radiates outside the confinement region
...up to 90% of the heating power

- exists above a power-dependent density threshold
- exists for detached plasma at target plates and up to density limit
- exists over large Bt range (0.9-2.5T)
- exists up to highest beta attained (3.4%)
- exists for hydrogen and deuterium plasmas, with “interesting differences“
- exists over a variety of magnetic configurations...including limiter-plasmas (high NBI)

Quasi-Axisymmetry Offers Innovative Solutions

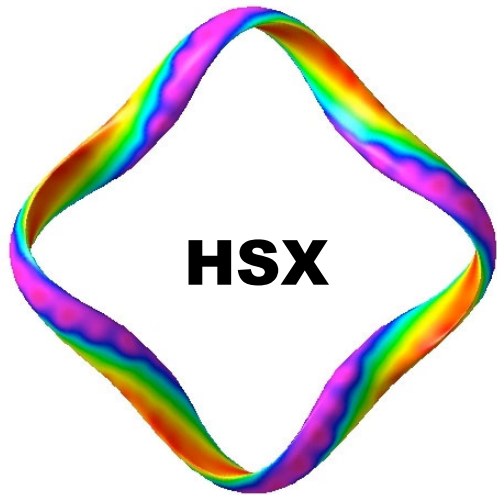
Use 3D shaping to:

- Quasi-axisymmetry to close orbits, allow flow, get good confinement
 - Take advantage of tokamak advances on transport control
 - Use bootstrap to raise iota
- Aspect ratio ~ 4
 - $n=0$ toroidal Fourier terms large
 - compatible with quasi-axisymmetry
- Passively stabilize external kink, vertical, neo-tearing, ballooning modes
 - expand safe operating area to $\beta \geq 4\%$,
without need for conducting walls or feedback systems
 - prevent disruptions?
- Steady state without current drive. Control of iota (q) and shear via coils

□ **NCSX Design Goals**

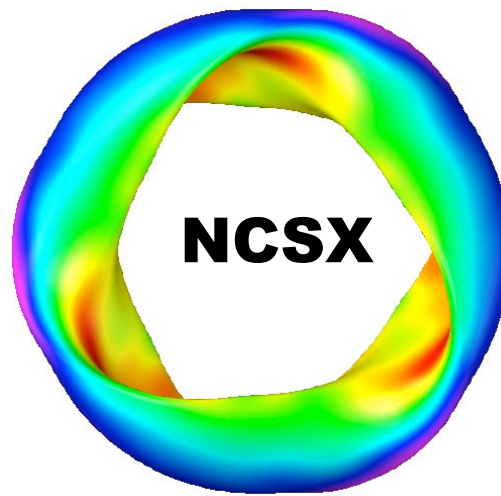
Using Advances in Theory and Numerical modeling; parallel computing
(NERSC, ACL/LANL, Princeton/PPPL)

Devices that test the 3 possible forms of quasi-symmetry are either operating or planned in the U.S.



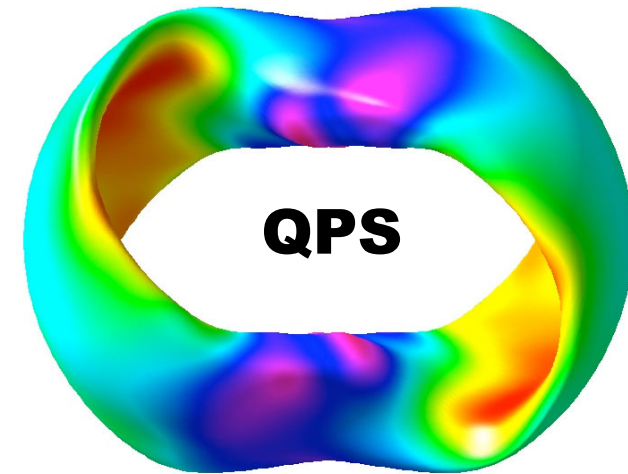
HSX

Univ. of Wisconsin



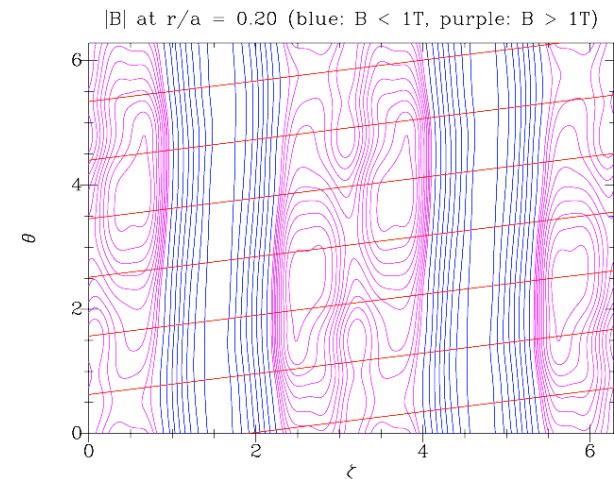
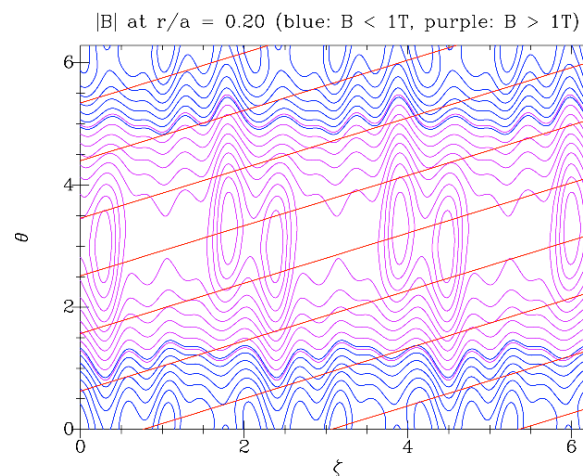
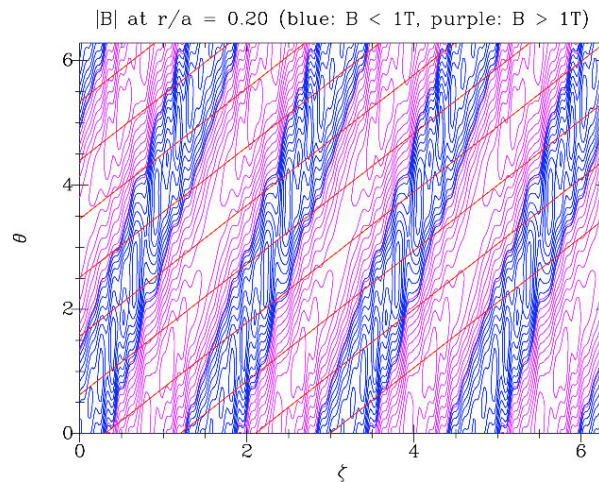
NCSX

*Princeton Plasma
Physics Lab.*

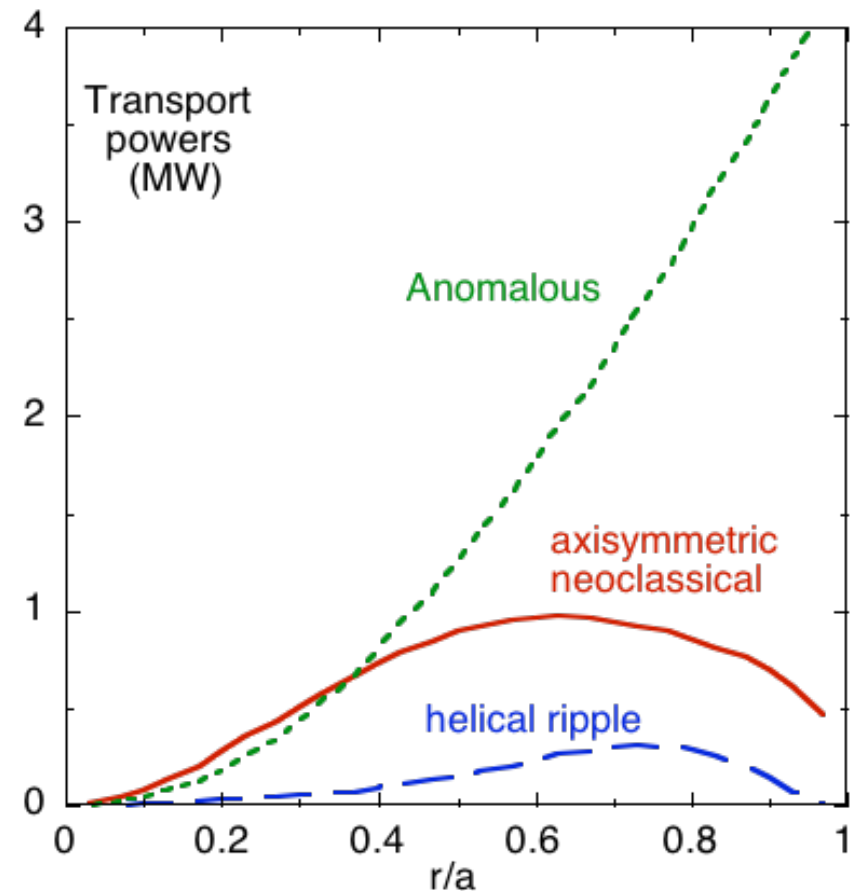
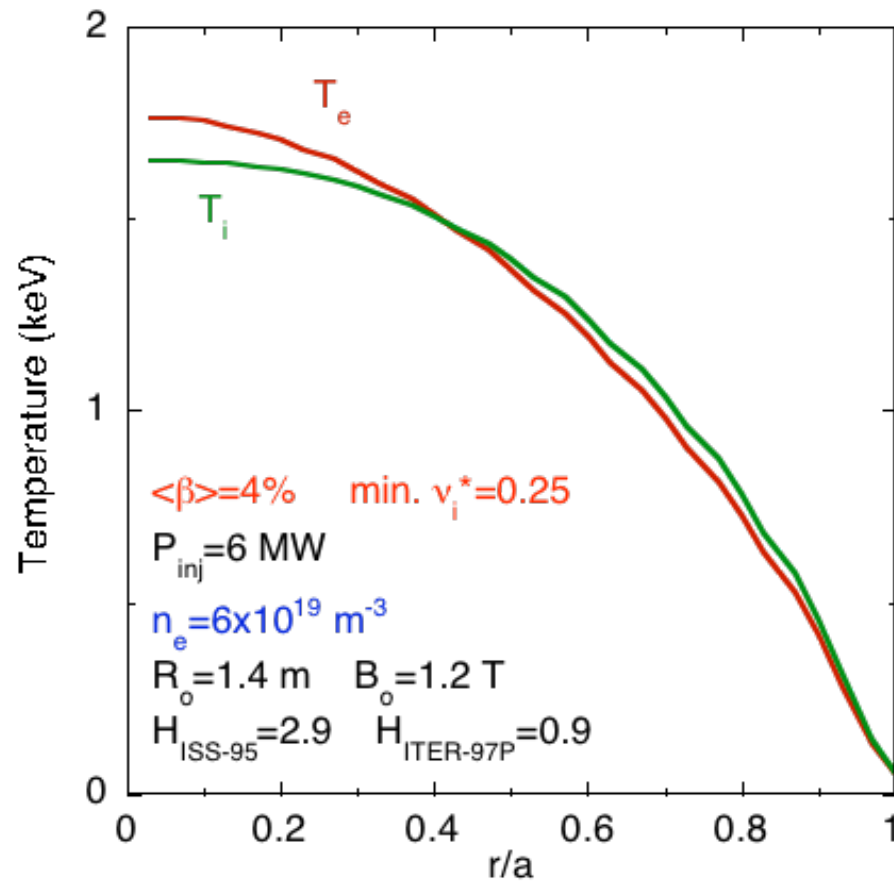


QPS

*Oak Ridge
National Lab.*



Low Helical Ripple Transport



- Total neoclassical transport dominates only for $r/a < 0.4$
- Neoclassical axisymmetric component $>$ helical ripple component
- Estimate of helical ripple transport assumes ambipolar E_r .

Transport Issues for NCSX

Helical neoclassical transport is not expected to be an important part of heat transport.
Axisymmetric neoclassical heat transport should be much larger.

Helical neoclassical transport may be the dominant source of viscosity.
Viscosity in tokamaks is low.

NBI-driven rotation will affect E_r :

it tends to drive E_r away from the ambipolar value for zero external torque,
this drives a radial current and the resulting $j_r \times B$ acts as a viscosity to damp rotation
neoclassical diffusion coefficients with rotating bulk plasma will be very different?

Ambient E_r will be enough to partially suppress microturbulence?

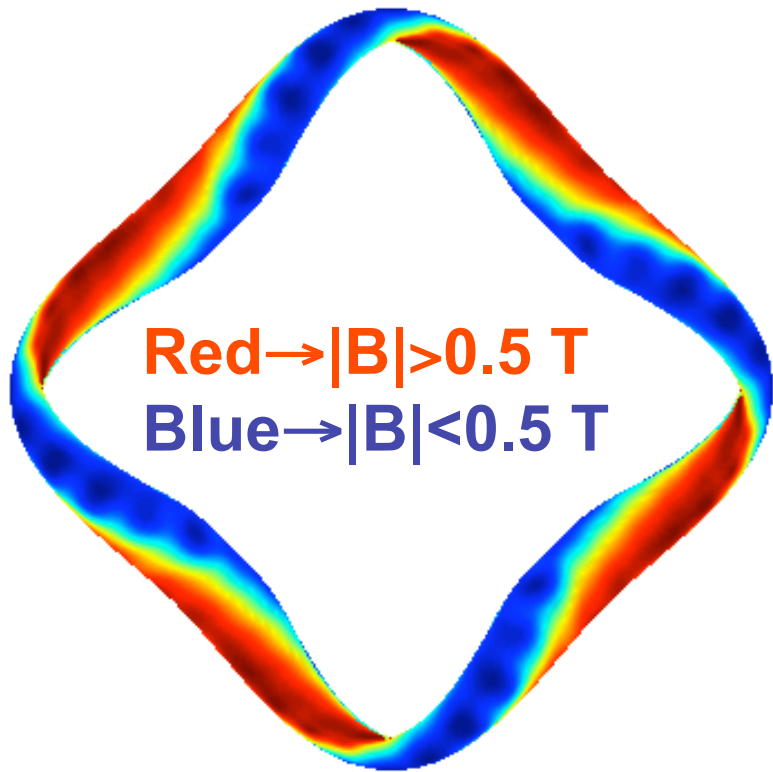
Ambient E_r will be enough to promote formation of transport barriers?

Low viscosity will allow formation of zonal flows?

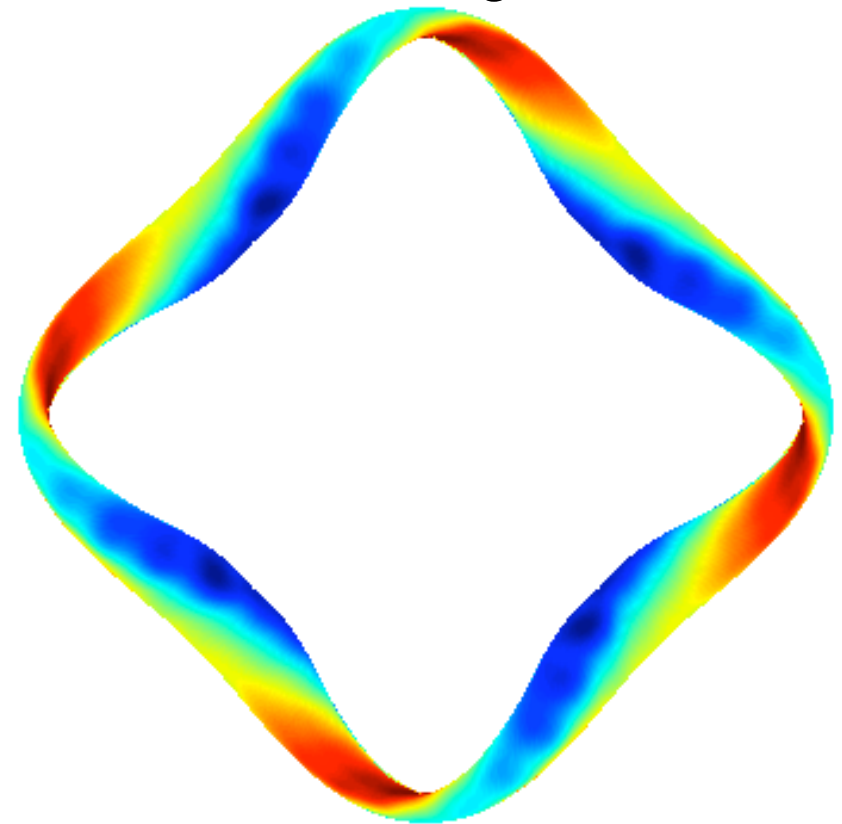
these will be strong enough to limit microturbulent transport as in tokamaks?

HSX is a Flexible Experiment for Studying Neoclassical Transport

QHS Configuration



Mirror Configuration



$B \sim 0.5$ T (1.2 T full design field)

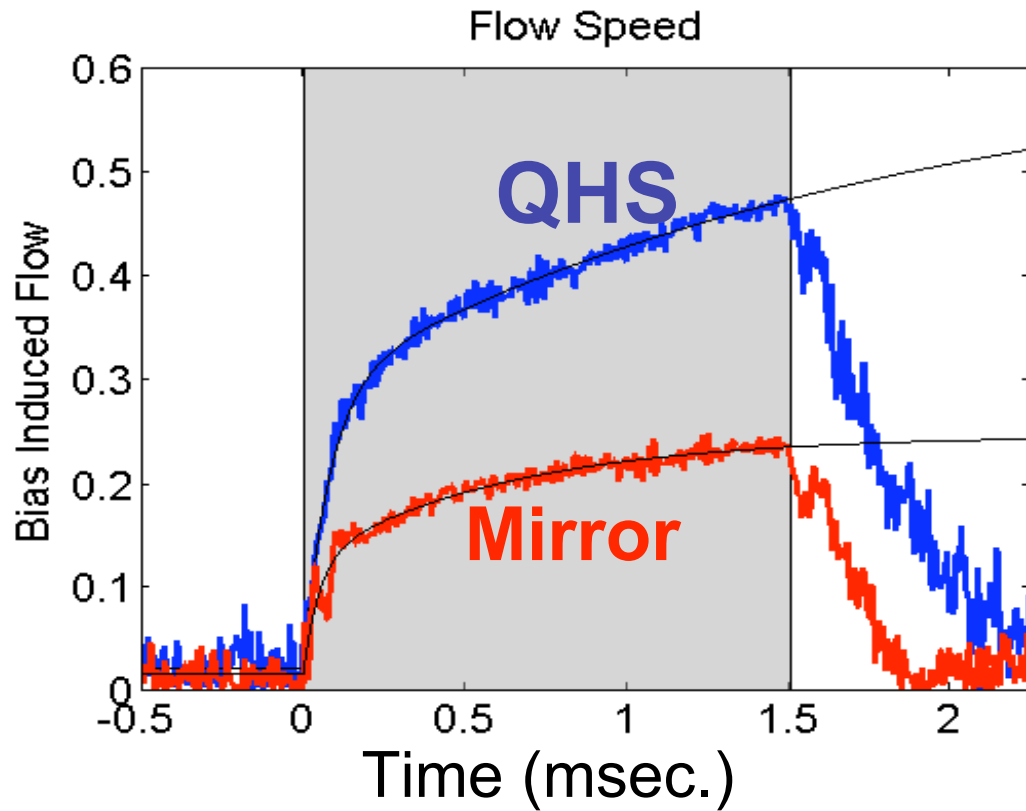
$P_{\text{ECH}} = 50$ kW (200 kW Gyrotron, exploring additional heating)

$R = 1.2$ m, $a \sim .12$ m

What was done...

- Studies of flow and electric field evolution
 - Asymmetries between the spin-up and relaxation
 - Two time-scale flow evolution
 - Reduced damping with quasisymmetry
- Neoclassical modeling of flow damping
 - Original model for the spin-up
 - Methods to compare predictions in “flux-coordinates” to lab-frame measurements.
- Measurements/modeling comparison
 - Reduced flow damping in quasisymmetric configurations
 - Flow damping larger than the neoclassical prediction

Preview: QHS Flows Damp More Slowly, Goes Faster For Less Drive



**QHS: 8 A of
electrode current**

**Mirror: 10 A of
electrode current**

All other parameters ($n_e = 1 \times 10^{12} \text{ cm}^{-3}$, $n_n \approx 1 \times 10^{10} \text{ cm}^{-3}$,
 $T_i \approx 25 \text{ eV}$, $B = 0.5 \text{ T}$, $P_{\text{ECH}} = 50 \text{ kW}$) held constant.